

# Atmospheric CO and CH<sub>4</sub> time series and seasonal variations on Reunion Island from ground-based in-situ and FTIR (NDACC and TCCON) measurements

Minqiang Zhou<sup>1</sup>, Bavo Langerock<sup>1</sup>, Corinne Vigouroux<sup>1</sup>, Mahesh Kumar Sha<sup>1</sup>, Michel Ramonet<sup>2</sup>, Marc Delmotte<sup>2</sup>, Emmanuel Mahieu<sup>3</sup>, Whitney Bader<sup>3</sup>, Christian Hermans<sup>1</sup>, Nicolas Kumps<sup>1</sup>, Jean-Marc Metzger<sup>4</sup>, Valentin Duflot<sup>5,4</sup>, Zhiting Wang<sup>6,7</sup>, Mathias Palm<sup>6</sup>, and Martine De Mazière<sup>1</sup>

<sup>1</sup>Royal Belgian Institute for Space Aeronomy (BIRA-IASB), Brussels, Belgium

<sup>2</sup>Laboratoire des Sciences du Climat et de l'Environnement (LSCE/IPSL), UMR CEA-CNRS-UVSQ, Gif-sur-Yvette, France

<sup>3</sup>Institut d'Astrophysique et de Géophysique, Université de Liège, Liège, Belgium

<sup>4</sup>UMS 3365 – OSU Réunion, Université de La Réunion, Saint-Denis, Réunion, France

<sup>5</sup>Laboratoire de l'Atmosphère et des Cyclones (LACy), UMR8105, Saint-Denis, Réunion, France

<sup>6</sup>Institute of Environmental Physics, University of Bremen, Bremen, Germany

<sup>7</sup>College of Atmospheric Science, Lanzhou University, Lanzhou 730000, China

*Correspondence to:* Minqiang Zhou (minqiang.zhou@aeronomie.be)

**Abstract.** Atmospheric carbon monoxide (CO) and methane (CH<sub>4</sub>) concentrations are measured by ground-based in-situ Cavity Ring-Down Spectroscopy (CRDS) analyzers and Fourier transform infrared (FTIR) spectrometers at two sites (St Denis and Maïdo) on Reunion Island (21°S, 55°E) in the Indian Ocean. Currently, the FTIR Bruker IFS 125HR at St Denis records the direct solar spectra in the near-infrared range, contributing to the Total Carbon Column Observing Network (TCCON).

5 The FTIR Bruker IFS 125HR at Maïdo records the direct solar spectra in the mid-infrared range, contributing to the Network for the Detection of Atmospheric Composition Change (NDACC). In order to understand the atmospheric CO and CH<sub>4</sub> variability on Reunion Island, the time series and seasonal cycles of CO and CH<sub>4</sub> from in-situ and FTIR (NDACC and TCCON) measurements are analysed. Meanwhile, the difference between the in-situ and FTIR measurements are discussed.

The CO seasonal cycles observed from the in-situ measurements at Maïdo and FTIR retrievals both at St Denis and Maïdo 10 are in good agreement with a peak in September-November, primarily driven by the emissions from biomass burning in Africa and South America. The dry-air column averaged mole fraction of CO ( $X_{CO}$ ) derived from the FTIR MIR spectra (NDACC) is about 15.7 ppb larger than the CO mole fraction near the surface at Maïdo, because the air in the lower troposphere mainly comes from the Indian Ocean while the air in the middle and upper troposphere mainly comes from Africa and South America. The trend for CO on Reunion Island is unclear during 2011-2017, and more data need to be collected to get a robust result.

15 A very good agreement is observed in the tropospheric and stratospheric CH<sub>4</sub> seasonal cycles between FTIR (NDACC and TCCON) measurements, and in-situ and the Michelson Interferometer for Passive Atmospheric Sounding (MIPAS) satellite measurements, respectively. In the troposphere, the CH<sub>4</sub> mole fraction is high in August-September and low in December-January, which is due to the OH seasonal variation. In the stratosphere, CH<sub>4</sub> concentration has its maximum in March-April and its minimum in August-October, which is dominated by vertical transport. In addition, the different CH<sub>4</sub> concentration between 20 the in-situ, NDACC and TCCON CH<sub>4</sub> measurements in the troposphere are discussed, and all measurements are in good

agreement with the GEOS-Chem model simulation. The trend of  $X_{CH_4}$  is  $7.6 \pm 0.4$  ppb/year from the TCCON measurements over the 2011-2017 time period, which is consistent with the  $CH_4$  trend of  $7.4 \pm 0.5$  ppb/year from the in-situ measurements for the same time period at St Denis.

## 1 Introduction

5 Carbon monoxide (CO) is a colorless and poisonous trace gas, which contributes significantly to the pollution of our planet. CO has a lifetime of several weeks to a few months (Novelli et al., 1998), therefore, it is generally used in atmospheric sciences as a tracer to study the long-distance transport of forest fire, biomass burning and other emissions (Duflot et al., 2010). CO also plays an important role in atmospheric chemistry, especially reacting with hydroxyl radicals (OH) which affect the carbon and the methane ( $CH_4$ ) cycles (Rasmussen and Khalil, 1981), and take part in the formation of many other polluting gases, e.g., 10 tropospheric ozone, and urban smog (Aschi and Largo, 2003).  $CH_4$  is the second most important anthropogenic greenhouse gas after carbon dioxide ( $CO_2$ ), with a global warming potential about 28 times greater than  $CO_2$  over a 100-year time horizon. About 17% of the total increase in radiative forcing between 1750 and 2010 related to the long-lived greenhouse gases in the atmosphere is caused by  $CH_4$  (IPCC, 2013). In addition,  $CH_4$  also reacts with OH, affecting the atmospheric oxidizing capacity.  $CH_4$  is well-mixed in the lower atmosphere with a life time of 8-10 years (Kirschke et al., 2013).

15 In recent decades,  $CH_4$  growth rates in the atmosphere have been variable. The  $CH_4$  concentration was increasing in the 1990s at rate of 0.7%/year, it was then relatively stable in the first half of the 2000s, but started increasing again after 2007 (Rigby et al., 2008). The CO concentration increased since the 1950s and then started to decrease in the late 1980s (Novelli, 2003). The importance of CO and  $CH_4$  in our changing atmosphere motivates continuous and long-term time series of precise and accurate measurements of these species. Several kinds of measurement techniques have been used to monitor the CO and 20  $CH_4$  concentrations in the atmosphere, e.g. ground-based in-situ or sampling measurements (Vermeulen et al., 2011; Lopez et al., 2015); ground-based Fourier Transform Infrared (FTIR) spectrometer observations (Sussmann et al., 2012; Té et al., 2016), and space-based satellite measurements such as the Michelson Interferometer for Passive Atmospheric Sounding (MIPAS), the Greenhouse gases Observing SATellite (GOSAT) and the Measurement Of Pollution In The Troposphere (MOPITT) (von Clarman et al., 2003; Yokota et al., 2009; Deeter et al., 2014). In addition of providing useful means for trend determination, such measurements allow the verification of atmospheric models for air pollution and climate change, e.g. Té et al. (2016) 25 used ground-based in-situ and FTIR measurements as well as GEOS-Chem simulations to explain the seasonal variability of atmospheric CO, and Bader et al. (2017) used FTIR measurements together with the GEOS-Chem model to investigate the possible causes for the recent increase of atmospheric  $CH_4$  since 2005.

Reunion Island is a unique atmospheric observatory situated in the Indian Ocean, about 700 km east of Madagascar and 30 170 km southwest of Mauritius. It is one of the very few atmospheric observation stations providing both in-situ and remote sensing FTIR CO and  $CH_4$  data in the Southern Hemisphere. Both in-situ and FTIR measurement techniques are capable of measuring CO and  $CH_4$  concentrations with high accuracy and precision, and are therefore good candidates to study the changes in atmospheric compositions, and to trace the emissions. However, using ground-based in-situ and FTIR measure-

ments requires a good understanding of the uncertainty and representativeness of each dataset. In-situ instruments monitor gas concentrations near the surface, while FTIR retrievals report information on the distribution of the gas abundance with altitude. The representativeness of both measurements depends on the location of the site, the air transport, and the lifetime of the target species (Folini et al., 2009; Dils et al., 2011; Sepúlveda et al., 2014). In addition, the representativeness of FTIR retrievals, 5 and their vertical sensitivity is also related to the spectral range and retrieval strategy, which has to be taken into account when comparing the Total Carbon Column Observing Network (TCCON) and the Detection of Atmospheric Composition Change (NDACC) data (Ostler et al., 2014; Kiel et al., 2016).

The objective of this paper is to study the atmospheric CO and CH<sub>4</sub> time series and seasonal variations on Reunion Island based on the in-situ and FTIR measurements from two sites, Saint Denis (St Denis) and Maïdo. The different techniques 10 of ground-based in-situ and FTIR (NDACC and TCCON) are used to show their complementarity, to obtain the CO and CH<sub>4</sub> abundances at the surface and in the troposphere and stratosphere. Sect. 2 introduces the datasets at the two sites. The measurement uncertainty and characterization of the various datasets are presented. In the next section, the time series and seasonal cycles of CO and CH<sub>4</sub> from the in-situ measurements at the surface and FTIR column retrievals are analysed. In addition, intercomparisons between co-located daily means of the in-situ and FTIR measurements are carried out. In Sect. 4, 15 the differences of CO and CH<sub>4</sub> between the in-situ and FTIR measurements are discussed by using the vertical information of the FTIR data which allows tropospheric columns to be derived, and by providing GEOS-Chem model comparisons for CH<sub>4</sub> in the troposphere. Furthermore, in Sect. 4, the FTIR CH<sub>4</sub> stratospheric columns are compared with MIPAS satellite data. Finally, conclusions are drawn in Sect. 5.

## 2 Measurements on Reunion Island

20 There are two sites on Reunion Island: St Denis (-20.9014 ° N, 55.4848 ° E; 85 m a.s.l. above sea level) close to the coast and Maïdo (-21.0796 ° N, 55.3841 ° E; 2155 m a.s.l.) close to the top of the mountain ridge. Table 1 lists all the available CO and CH<sub>4</sub> measurements from these two sites, together with their measurement uncertainties. Currently, each site is operated with a FTIR instrument and an in-situ Cavity Ring-Down Spectroscopy (CRDS) analyzer. In this section, we give a brief historic overview of the in-situ and the FTIR measurements on Reunion Island.

### 25 2.1 In-situ

The Royal Belgian Institute for Space Aeronomy (BIRA-IASB) in collaboration with the Laboratoire de l'Atmosphère et des Cyclones (LACy), the Observatoire des Sciences de l'Univers de la Réunion (OSU-R) and the Laboratoire des Sciences du Climat et de l'Environnement (LSCE), has performed in-situ surface measurements on Reunion Island. CH<sub>4</sub> mole fraction has been measured by a CRDS analyzer (Picarro G1301) at St Denis since August 2010, and CO and CH<sub>4</sub> mole fractions 30 have been collected by another CRDS analyzer (Picarro G2401) at Maïdo since December 2014. The latter installation will be proposed in late 2018 for a certification (to be certified for standardized data production) in the European research infrastructure Integrated Carbon Observation System (ICOS-ERIC) as a French-Belgian station. The St Denis coastal site has been developed

**Table 1.** In-situ and FTIR CO and CH<sub>4</sub> measurements at St Denis and Maïdo.

Site	St Denis			Maïdo	
Location	-20.9014 N, 55.4848 E			-21.0796 N, 55.3841 E	
Altitude	85 m a.s.l.			2155 m a.s.l.	
Instrument	FTIR IFS 120M	FTIR IFS 125HR	Picarro G1301	FTIR IFS 125HR	Picarro G2401
Time coverage	2002.10 – 2011.11	2011.9 –	2010.8 –	2013.3 –	2014.1 –
Network	NDACC	TCCON	French atmospheric monitoring network	NDACC	ICOS applicant
CO uncertainty*	2.7 / 1.2 %	- / 1.2 %	–	2.5 / 1.0 %	- / 1.5 ppb
CH <sub>4</sub> uncertainty*	3.5 / 1.6 %	- / 0.5 %	- / 2.0 ppb	3.0 / 1.5 %	- / 0.5 ppb

\* FTIR uncertainty is given in percentage, while in-situ uncertainty is in absolute unit of VMR. NDACC uncertainty is reported on the total column, and it is separated into two components (systematic / random). TCCON uncertainty is reported on the total column-averaged mole fraction. Because TCCON and in-situ measurements have been validated under WMO standards, it is assumed there are no systematic uncertainties for these data.

within the French national monitoring network. The two stations have been set up in a similar way, taking into account the technical specifications recommended by ICOS (Laurent, 2016). Both CRDS analyzers are calibrated every 3 to 4 weeks with a suite of four cylinders whose concentrations, spanning the atmospheric ranges of CH<sub>4</sub> and CO, have been calibrated at LSCE with NOAA reference tanks. All values are expressed in WMO reference scales (X2004A and X2014A for CH<sub>4</sub> and CO 5 respectively). In addition, those tanks are used to calculate the continuous monitoring repeatability (CMR) and the long-term repeatability (LTR) as defined by Yver Kwok et al. (2015). The air is sampled through a 1/4" tube ('Synflex 3000') at the top of the building, and then goes through a 2 $\mu$ m filter, and a multi-position valve before being analyzed by the CRDS analyzer. The pump is always located downstream of the analyzer. Raw data are transferred every night to the LSCE server, and are processed according to the ICOS specifications (Hazan et al., 2016). The in-situ measurements at the two surface sites are 10 done in wet conditions without any dryer in the sampling line. The correction to dry air mole fractions is done using the H<sub>2</sub>O measurements performed by the same analyzers (Rella et al., 2013).

## 2.2 FTIR – Instruments

In 2002 (October) and 2004 (August to November), BIRA-IASB carried out two atmospheric monitoring experiments, using a mobile Bruker IFS 120M FTIR, equipped with indium antimonide (InSb) and mercury cadmium telluride (MCT) detectors at 15 St Denis on the campus of the Université de La Réunion (Senten et al., 2008). The same instrument was operated at St Denis to provide continuous measurements between June 2009 and November 2011 (Vigouroux et al., 2012; Zhou et al., 2016). The instrument recorded the solar spectra in the mid-infrared (MIR) range from 600-4500 cm<sup>-1</sup>, contributing to the NDACC network.

In September 2011, BIRA-IASB installed a high-resolution Bruker IFS 125HR FTIR at St Denis next to the FTIR 120M. The instrument is dedicated primarily to measure the near-infrared (NIR: 4000-16000  $\text{cm}^{-1}$ ) spectra with silicon (Si) and indium gallium arsenide (InGaAs) detectors, contributing to TCCON.

In March 2013, BIRA-IASB started operating a second Bruker IFS 125HR FTIR spectrometer, observing the MIR spectra 5 with MCT and InSb detectors at the Maïdo observatory (Baray et al., 2013). These FTIR measurements are also affiliated with NDACC.

### 2.3 FTIR – retrieval techniques

The optimal estimation method (Rodgers, 2000) is applied to retrieve the gas concentrations from the FTIR solar spectra. The retrieval strategies are determined by the spectral range and the network (see Table 2).

**Table 2.** NDACC and TCCON CO and  $\text{CH}_4$  retrieval strategies for data recorded on Reunion Island.

Species	CO		$\text{CH}_4$	
Network	TCCON	NDACC	TCCON	NDACC
Algorithm	GGG2014	SFIT4	GGG2014	SFIT4
Retrieval windows ( $\text{cm}^{-1}$ )	4208.7-4257.3	2057.7-2058.0	5872.0-5988.0	2611.6-2613.35
	4262.0-4318.8	2069.56-2069.76	5996.45-6007.55	2613.7-2615.4
		2157.5-2159.15	6007.0-6145.0	2835.55-2835.8
				2903.82-2903.925
				2941.51-2942.22
Interfering species	$\text{CH}_4, \text{H}_2\text{O}, \text{HDO}$	$\text{O}_3, \text{N}_2\text{O},$ $\text{H}_2\text{O}, \text{OCS}, \text{CO}_2$	$\text{CO}_2, \text{H}_2\text{O}, \text{N}_2\text{O},$	$\text{H}_2\text{O}, \text{HDO},$ $\text{CO}_2, \text{NO}_2$
Spectroscopy	ATM	ATM	ATM	DLR $\text{H}_2\text{O}$ , ATM
A priori profile	TCCON tool (daily)	WACCM v4 (fixed)	TCCON tool (daily)	WACCM v4 (fixed)
Retrieval constraint	scaling of a priori profile	optimal estimation	scaling of a priori profile	optimal estimation
		DOF=2.0±0.2 (St Denis)	file	DOF=2.1±0.2 (St Denis)
		DOF=2.3±0.2 (Maïdo)		DOF=2.5±0.3 (Maïdo)
Products	total column	profile	total column	profile

#### 10 2.3.1 TCCON

The TCCON (NIR) spectra at St Denis are analysed using the GGG2014 algorithm to retrieve CO and  $\text{CH}_4$  total columns (De Maziere et al., 2017). The details of the TCCON retrieval settings were described in Wunch et al. (2015). Note that GGG2014 applies a profile scaling, therefore TCCON only provides a total column instead of a vertical profile. The daily a priori profiles are generated by a stand alone tool based on in-situ and aircraft measurements (Toon and Wunch, 2014). Figure

1 shows the a priori profiles of CO and CH<sub>4</sub> at St Denis on four days in 2013. TCCON CO and CH<sub>4</sub> retrieved products have been calibrated and validated by Infrastructure for the Measurement of the Europe Carbon Cycle (IMECC) profiles over the European TCCON stations (Messerschmidt et al., 2011) and HIAPER Pole-to-Pole Observations (HIPPO) profiles over Northern America, East Asia and Oceania (Wunch et al., 2010), and the calibration factors (CO:  $1.067 \pm 0.020$ ; CH<sub>4</sub>: 5  $0.977 \pm 0.002$ ) are found to be robust both over time and from site to site (Wunch et al., 2015). The data in this study have all been corrected by applying these calibration factors. Therefore, it is assumed that there are no systematic uncertainties for the TCCON retrievals and hence only random uncertainties are listed in Table 1.

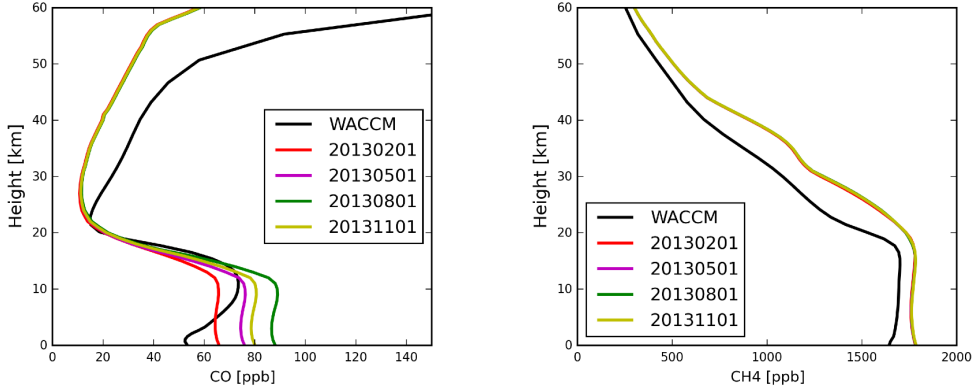


**Figure 1.** The a priori profiles used for TCCON measurements on 20130201 (year month day), 20130501, 20130801, 20131101 and NDACC measurements for CO (left) and CH<sub>4</sub> (right). Note that NDACC uses a fixed a priori profile from WACCM model for all retrievals.

Figure 2 shows the column averaging kernels (AVK) of TCCON CO and CH<sub>4</sub> retrievals for different Solar Zenith Angles (SZAs). At St Denis, the SZA is mainly in the range of 20-70 °. The AVK represents the sensitivity of the retrieved total column 10 to the true partial column profile. Ideally, the AVK should be 1.0 at all altitudes, meaning that the retrieved total column is the same as the true one, with a perfect sensitivity to the whole atmosphere. However, in reality, the AVK is not always equal to 1.0. If the value is larger than 1.0 at one altitude, it means that the retrieved total column overestimates the contribution from that particular layer in the total column budget, and vice versa. As a result, TCCON retrieved CO total column underestimates a deviation from the a priori in the lower troposphere, and overestimates it at high altitudes. TCCON retrieved CH<sub>4</sub> total column 15 is more sensitive to the whole troposphere and stratosphere.

### 2.3.2 NDACC

The NDACC (MIR) spectra at St Denis and Maïdo are analysed with the SFIT4 algorithm, an evolution of SFIT2 (Pougatchev et al., 1995), to retrieve the profiles of CO and CH<sub>4</sub>. The H<sub>2</sub>O a priori profile is extracted from the National Centers for Environmental Prediction (NCEP) 6-hourly re-analysis data, and a priori profiles of other species are derived from the Whole 20 Atmosphere Community Climate Model (WACCM) version 4 (see Figure 1). In order to reduce the influence from the inter-

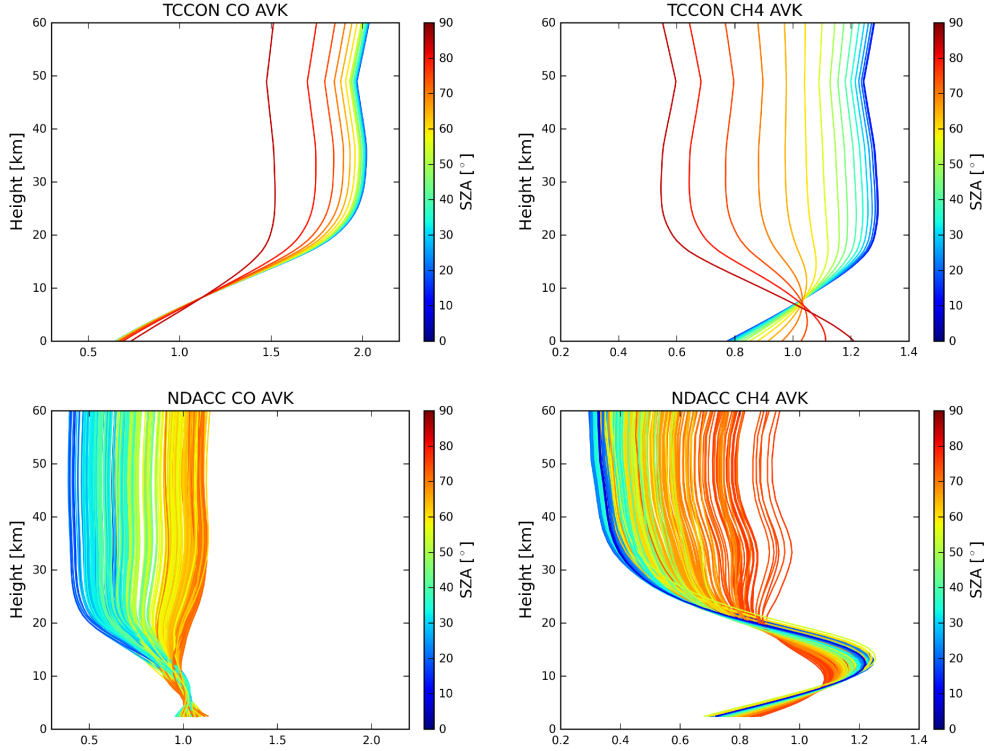


**Figure 2.** Upper panels: the column averaging kernels of TCCON CO (left) and CH<sub>4</sub> (right) retrievals; Lower panels: the column averaging kernels of NDACC CO (left) and CH<sub>4</sub> (right) retrievals. All averaging kernels vary with the SZA. Note that the ranges of x axis for CO and CH<sub>4</sub> are different.

fering species, profiles of O<sub>3</sub> and N<sub>2</sub>O and columns of H<sub>2</sub>O, OCS and CO<sub>2</sub> are simultaneously retrieved together with the CO profile (see Table 2). Profiles of H<sub>2</sub>O and HDO, and columns of CO<sub>2</sub> and NO<sub>2</sub> are simultaneously retrieved together with the CH<sub>4</sub> profile. The retrieval uncertainty of NDACC retrievals at Maïdo is slightly lower than that at St Denis, because of the higher Signal-to-Noise-Ratio (SNR) of the FTIR 125HR compared to the FTIR 120M. In addition, the H<sub>2</sub>O at Maïdo is less significant than that at St Denis due to the higher altitude, which is an important interfering species for CO and CH<sub>4</sub> retrievals. The NDACC retrievals are performed using the same atmospheric line list (ATM) (Toon, 2014) as used by TCCON with the exception of the H<sub>2</sub>O line list. The latest H<sub>2</sub>O line list (Birk et al., 2017; Loos et al., 2017a, b) provided by the German Aerospace Center (DLR) in 2016 is adopted for NDACC CH<sub>4</sub> retrievals, which allows us to get a better spectral fitting.

The AVK for NDACC CO and CH<sub>4</sub> retrievals are shown in Figure 2. Similar to TCCON, NDACC CO and CH<sub>4</sub> AVK vary with SZA. NDACC CO retrievals have a good sensitivity to the whole troposphere and lower stratosphere. For CH<sub>4</sub>, the total column is sensitive to the whole troposphere and stratosphere. Apart from the total column, NDACC provides some profile information of CO and CH<sub>4</sub>. Figure 3 shows a typical AVK of CO and CH<sub>4</sub> NDACC retrievals at Maïdo. The averaged Degrees

Of Freedom for signal (DOFs) of CO is  $2.0 \pm 0.2$  ( $1\sigma$ ) at St Denis and  $2.3 \pm 0.2$  ( $1\sigma$ ) at Maïdo, indicating that there are two individual layers of information (surface-8 km and 8-20 km) with the first layer having a strong sensitivity to the boundary layer. For CH<sub>4</sub>, the averaged DOFs of CH<sub>4</sub> is  $2.1 \pm 0.2$  ( $1\sigma$ ) at St Denis and  $2.5 \pm 0.3$  ( $1\sigma$ ) at Maïdo, indicating that there are also two individual layers of information (about surface-16 km and 16-60 km).

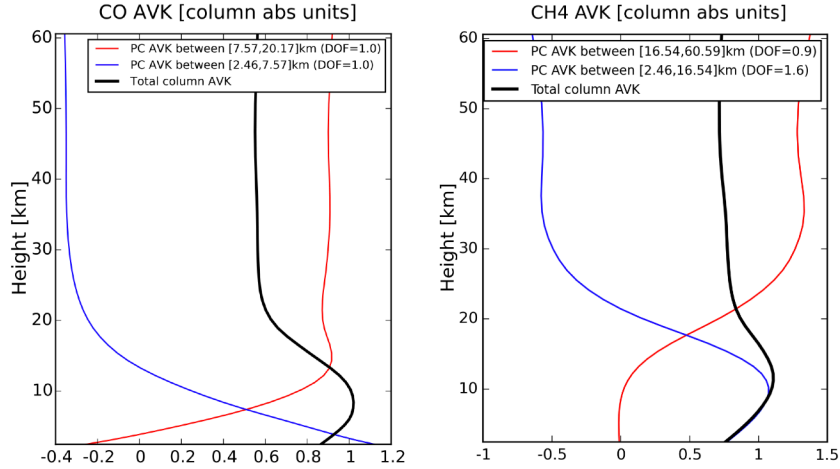


**Figure 3.** The total column averaging kernel (black), together with the partial column averaging kernels of two individual layers (CO: surface-8 km and 8-20 km; CH<sub>4</sub>: surface-16 km and 16-60 km) of one typical NDACC retrieval at Maïdo.

## 5 3 Comparison between the ground-based in-situ and the FTIR total column measurements

### 3.1 Methodology

In this section, we compare the CO and CH<sub>4</sub> dry air volume mixing ratio (VMR) observed by in-situ measurements at the surface, with the dry-air column-averaged mole fractions ( $X_{gas}$ ) of FTIR (NDACC and TCCON) retrievals. For TCCON products, O<sub>2</sub> total column is simultaneously retrieved with the target species. Since atmospheric O<sub>2</sub> concentrations are considered stable with the VMR of 0.2095, the  $X_{gas}$  is calculated by using the ratio between the total column of target species ( $TC_{gas}$ ) and O<sub>2</sub> ( $TC_{O_2}$ )

$$X_{gas} = 0.2095 \frac{TC_{gas}}{TC_{O_2}}. \quad (1)$$

The advantage of dividing by O<sub>2</sub> abundance is that it reduces the systematic uncertainties from the parameters, which have a similar effect on the retrievals of both species, e.g. instrument line shape (ILS) and the SZA (Yang et al., 2002). For NDACC spectra, there are no N<sub>2</sub> or O<sub>2</sub> absorption windows that allow to achieve a sufficient accuracy of abundance. Therefore, we use the dry-air total column ( $TC_{air}^{dry}$ ) to calculate the  $X_{gas}$

$$X_{gas} = \frac{TC_{gas}}{TC_{air}^{dry}}, \quad (2)$$

$$TC_{air}^{dry} = \frac{P_s}{gm_{air}^{dry}} - TC_{H_2O}(m_{H_2O}/m_{air}^{dry}), \quad (3)$$

where  $P_s$  is the surface pressure;  $g$  is the column-averaged gravitational acceleration;  $m_{H_2O}$  and  $m_{air}^{dry}$  are the molecular mass of  $H_2O$  and dry air, respectively;  $TC_{H_2O}$  is the total column of  $H_2O$  from NCEP re-analysis data. The surface pressures at St Denis and Maïdo are recorded by Vaisala PTB210 sensors, with an accuracy better than 0.1 hPa. The systematic uncertainty of  $H_2O$  in the troposphere is about 5%, and the  $TC_{H_2O}$  on Reunion Island is about 0.5-2 % of the  $TC_{air}$ . Consequently, the uncertainty of the  $TC_{air}^{dry}$  is less than 0.1%.

A regression model is applied to derive the trends of CO and  $CH_4$ , which has been described in Zhou et al. (2018).

$$Y(t) = A_0 + A_1 \cdot t + \sum_{k=1}^3 (A_{2k} \cos(2k\pi t) + A_{2k+1} \sin(2k\pi t)) + \varepsilon(t), \quad (4)$$

where  $A_0$  is the intercept;  $A_1$  is the annual growth rate;  $A_2$  to  $A_7$  are the periodic variations;  $\varepsilon(t)$  is the residual between the measurements and the fitting model;  $Y(t)$  is measurements with the  $t$  in fraction of year. After that, the detrended monthly means of the measurements are applied to obtain the seasonal variation, together with the uncertainty ( $2\sigma/\sqrt{n}$ ;  $\sigma$  and  $n$  being the standard deviation and the number of the measurements for each month).

For more quantitative comparisons, we also use the co-located daily means from the in-situ and FTIR measurements at each site (St Denis:  $CH_4$ ; Maïdo: CO and  $CH_4$ ). Note that the FTIR instrument measures direct sunlight, and it depends on clear sky conditions. Therefore we filter the in-situ measurements to daytime measurements (6:00-18:00; local time) to reduce the impact of the diurnal variation.

### 3.2 CO

The time series and seasonal cycle of CO from the in-situ and FTIR measurements are shown in Figure 4-5. For each dataset, we use all the available data to get a robust detrended time series and then to obtain the seasonal cycle. Figure 4 shows that the TCCON  $X_{CO}$  at St Denis is in good agreement with the NDACC  $X_{CO}$  at Maïdo, while the in-situ CO observations at Maïdo are generally lower than the FTIR measurements with the exception of few higher peaks. There is no distinct  $X_{CO}$  trend derived from both FTIR datasets (TCCON:  $-0.09 \pm 1.1$  ppb/year ( $2\sigma$ ) for 2011-2017; NDACC:  $-1.16 \pm 2.08$  ppb/year for 2013-2017), while a slight decreasing trend ( $-4.66 \pm 3.16$  ppb/year) for 2015-2017 is derived from the in-situ measurements. The large uncertainty of the decreasing trend is due to the limited time coverage (about 2.5 years), and the signal may be due to year-to-year variability. More data need to be collected to investigate the trend of CO on Reunion Island. Figure 5 shows that the seasonal cycles of CO from the in-situ and FTIR measurements are very similar with the maximum in September-November and minimum in February-April. The peak-to-peak amplitudes from NDACC and TCCON retrievals are very close ( $\sim 25-28$  ppb), and slightly weaker than the one from the in-situ measurements ( $\sim 32$  ppb). The high value corresponds to the period when the Island is downwind of emissions coming from the biomass burning in Africa and South America (Duflot et al., 2010; Vigouroux et al., 2012).

The time series and the correlation between the co-located in-situ and NDACC daily means of CO measurements at Maïdo are shown in Figure 6. There are 448 data pairs. The daily standard deviation of the in-situ measurements is larger than that of the NDACC retrievals. The difference (mean and standard deviation) between NDACC retrieved  $X_{CO}$  and in-situ CO is  $15.69 \pm 10.02$  ppb, which is beyond the systematic uncertainty of the NDACC retrievals (2-3 ppb). The correlation coefficient 5 (R) between the NDACC and in-situ measurements is 0.76. The slope (< 1.0) indicates that the absolute difference between the in-situ and NDACC measurements is large/small for the low/high CO values.

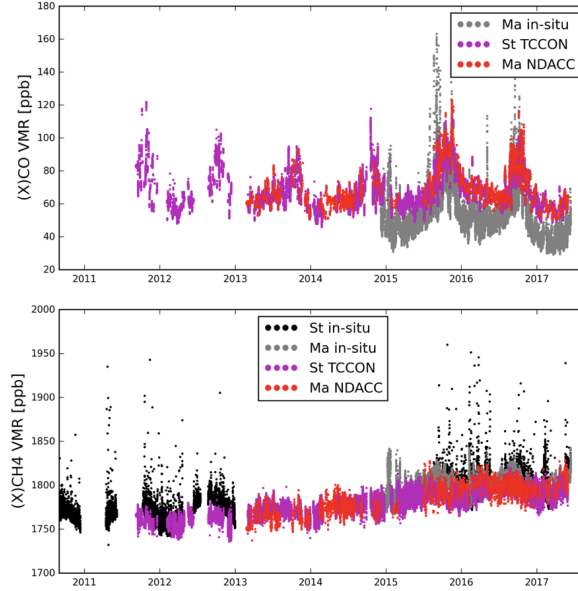


**Figure 4.** The time series of CO (upper) and CH<sub>4</sub> (lower) from in-situ and FTIR (NDACC and TCCON) measurements at St Denis and Maïdo. Note that, there is no CO in-situ measurement at St Denis. “St” and “Ma” in the labels represent St Denis and Maïdo, respectively. “(X)gas” is used in the ylabel for presenting in-situ VMR measurements and FTIR  $X_{gas}$  retrievals together.

### 3.3 CH<sub>4</sub>

A clear positive trend for CH<sub>4</sub> is recognized in Figure 4. The CH<sub>4</sub> annual growth is  $7.6 \pm 0.4$  ppb/year for the TCCON measurements for 2011-2017, and  $7.4 \pm 0.5$  ppb/year for the in-situ measurements for the same time period at St Denis. Both estimations 10 (at the surface and through the column) of the annual growth rates are in agreement with CH<sub>4</sub> trends observed at other locations after 2007 (Rigby et al., 2008; Bader et al., 2017). Although there is also a positive trend ( $\sim 5.4$  ppb/year) for the TCCON a priori CH<sub>4</sub>, it has a weak effect on the trend of retrieved CH<sub>4</sub> since TCCON has a good sensitivity to the atmosphere, especially in the troposphere (see Figure 2). The CH<sub>4</sub> annual growth is  $9.2 \pm 0.8$  ppb/year from the NDACC retrievals for 2013-2017, and the annual growth of the TCCON measurements is  $7.9 \pm 0.4$  ppb/year for the same time period. The annual growth of CH<sub>4</sub> in 15 2013-2017 is slightly larger than that in 2011-2017, which is consistent with the results from the NOAA/ESRL cooperative

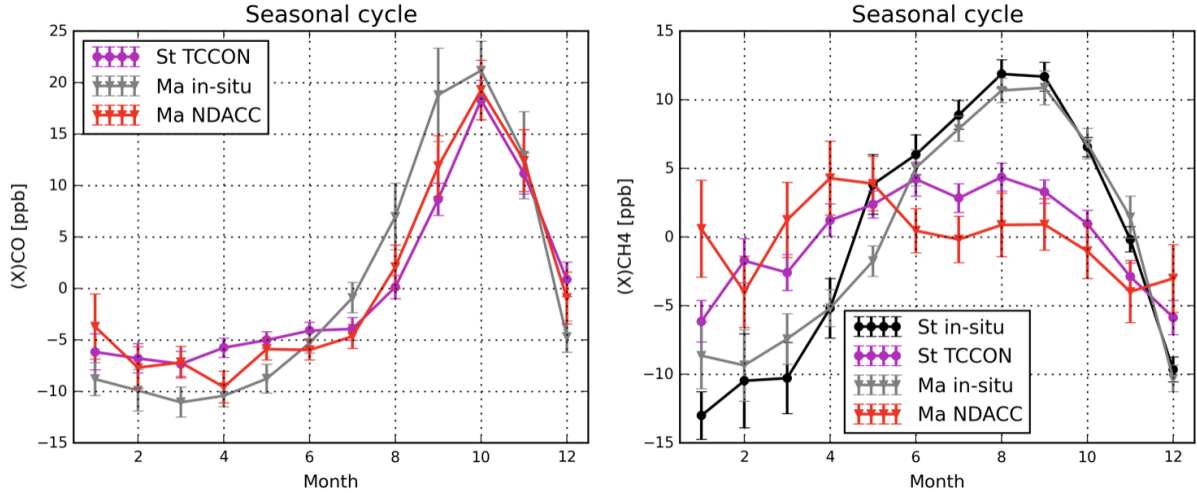


**Figure 5.** The seasonal cycles of CO (left) and CH<sub>4</sub> (right) from in-situ and FTIR (NDACC and TCCON) measurements at St Denis and Maïdo. The errorbar is  $1\sigma$  for all the detrended data within that month.

global air sampling network ([www.esrl.noaa.gov/gmd/ccgg/trends\\_ch4/](http://www.esrl.noaa.gov/gmd/ccgg/trends_ch4/)). The globally averaged marine surface CH<sub>4</sub> annual increases from NOAA/ESRL sites are  $7.7 \pm 0.6$  ppb/year in 2011-2017 and  $8.8 \pm 0.7$  ppb/year in 2013-2017.

The seasonal cycles of CH<sub>4</sub> from the in-situ measurements at St Denis and Maïdo are very close with the minimum in December-February and the maximum in August-September (see Figure 5). This corresponds to the seasonal variation of OH radicals, which are the major sink of CH<sub>4</sub> in the atmosphere (Kirschke et al., 2013). The seasonal cycles from the NDACC and TCCON retrievals are also similar, but different from the ones of the in-situ measurements. Both NDACC and TCCON X<sub>CH<sub>4</sub></sub> retrievals show high values in April-September and low values in October-March, but the seasonal cycle of X<sub>CH<sub>4</sub></sub> from NDACC retrievals has a small peak in March-May. The amplitude of the seasonal cycle from the in-situ measurements (about  $\pm 10$  ppb) is about 2 times larger than that from the FTIR measurements (about  $\pm 5$  ppb). The reasons for the different seasonal patterns between FTIR and in-situ are discussed in Sect. 4.

The time series and the correlation between the co-located in-situ and TCCON daily means of CH<sub>4</sub> measurements at St Denis are shown in Figure 7. The mean and standard deviation of the differences between the in-situ and TCCON measurements are -6.63 ppb and 9.78 ppb, respectively. The standard deviation of 9.78 ppb is almost within the combination of the random uncertainties of the TCCON retrievals ( $\sim 9$  ppb) and of the in-situ measurements ( $\sim 1$  ppb). Since there are no systematic uncertainties for both datasets, the mean value of -6.63 ppb is the difference between CH<sub>4</sub> VMR at surface and the total column averaged CH<sub>4</sub> at St Denis. As there is a distinct positive annual growth for CH<sub>4</sub> for 2011-2017, the correlation plot is labelled with the measurement year. The R between the TCCON X<sub>CH<sub>4</sub></sub> and in-situ CH<sub>4</sub> measurements is 0.86 for all the data pairs. However, if we only take the data pairs after 2015, the R value drops to 0.48.

The time series and the correlation between the co-located in-situ and NDACC daily means at Maïdo are shown in Figure 8. The averaged daily standard deviation of NDACC retrievals is larger than that of in-situ measurements, which is mainly due

to the larger random error of NDACC retrievals (see Table 1). The mean and standard deviation of the differences between the in-situ and FTIR measurements are 0.62 ppb and 11.90 ppb, respectively. The difference also shows a distinct seasonal variation. The R between daily NDACC  $X_{CH_4}$  and in-situ surface  $CH_4$  measurements is only 0.23. The lower correlation value is believed to be caused by the limited number of co-located measurements ( $\sim 2$  years) and by the fact that NDACC  $CH_4$  has 5 a reduced sensitivity to the boundary layer and an increased sensitivity to the stratosphere compared to the CO product.

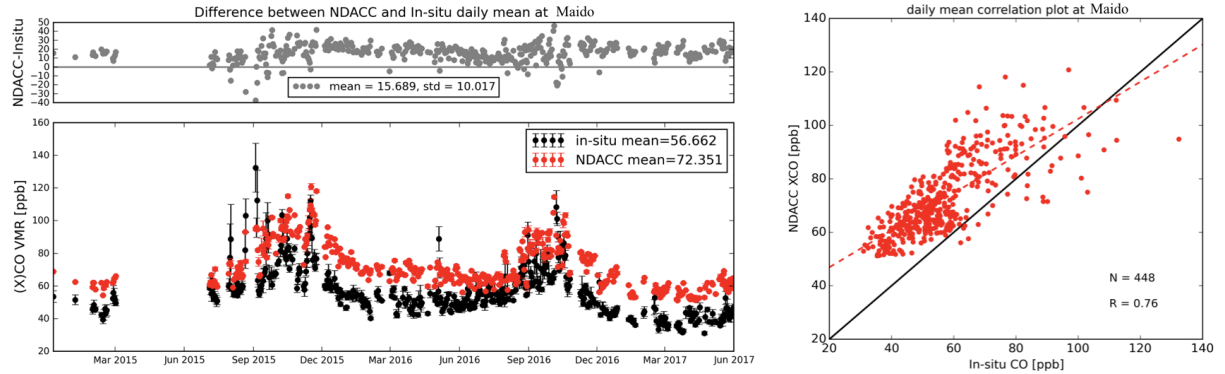


**Figure 6.** The time series of the daily means and standard deviations from FTIR (NDACC)  $X_{CO}$  and daytime in-situ CO measurements at Maido, together with the absolute difference (unit: ppb) between them (left lower and top, respectively) and their correlation (right).

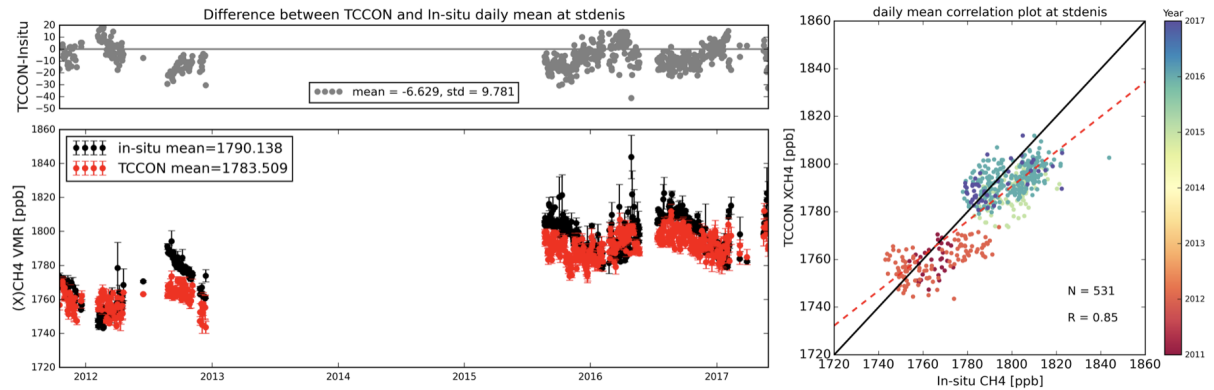


**Figure 7.** The time series of the daily means and standard deviations from the daytime in-situ and FTIR (TCCON)  $CH_4$  measurements at St Denis, together with the absolute difference (unit: ppb) between them (left lower and top, respectively) and their correlation (right). Since there is a distinct annual growth for  $CH_4$ , the dots are coloured according to the measurement year in the right panel.

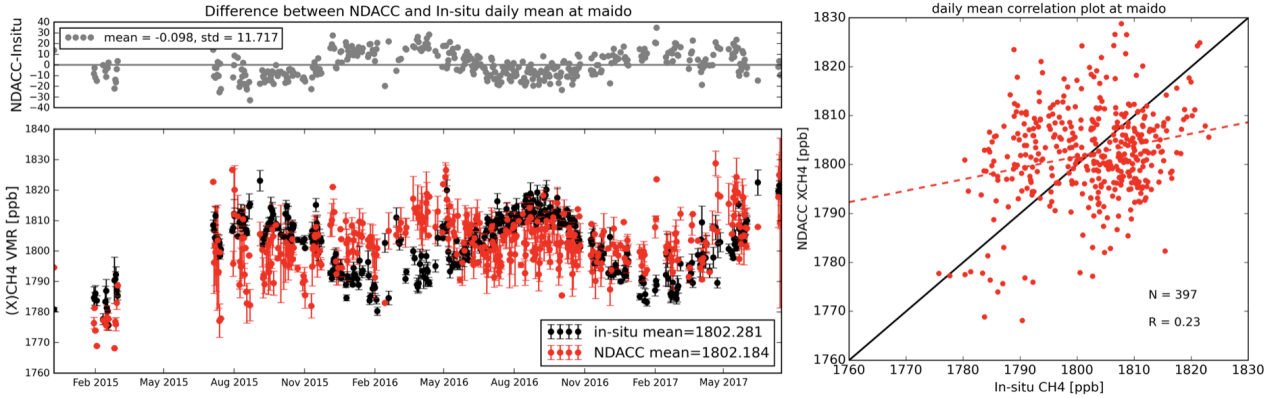


**Figure 8.** The time series of the daily means and standard deviations from the daytime in-situ and FTIR (NDACC)  $\text{CH}_4$  measurements at Maïdo, together with the absolute difference (unit: ppb) between them (left lower and top, respectively) and their correlation (right).

## 4 Discussions

### 4.1 CO

Atmospheric CO is mainly produced by the incomplete or inefficient combustion of carbon-based fuels (Kasischke and Bruhwiler, 2002) and the oxidation of methane or other carbon-containing compounds (Cullis and Willatt, 1983). Maïdo observatory being located on a remote mountain has weak direct anthropogenic CO emission nearby (European Commission, 2011), and very few spikes of in-situ measurements are observed in non-biomass-burning seasons (see upper panel in Figure 4 and Figure 6). Therefore, the CO molecules above Maïdo are either generated from oxidation processes in the atmosphere or transported from other places. The FLEXible PARTicle dispersion model (FLEXPART) v9.02 (Stohl et al., 2005) backward simulations (see Figure A1) are employed to understand the sources of air on Reunion Island. The settings of the FLEXPART run in this study are described in appendix A. The results are consistent with Figure 8 in Duflot et al. (2010). The air near the surface above Reunion Island is mainly coming from the Indian Ocean and partly from Southern Africa, and the air mass in the middle and upper troposphere is mainly coming from Africa and South America. As CO emission on the land is much larger than that from the ocean, this leads to the fact that FTIR  $X_{CO}$  is systematically larger than the in-situ CO at the surface.

As we mentioned in Sect. 2.3.2, the NDACC retrievals provide CO profiles, and there are about two individual layers of information (left panel in Figure 3). We calculate the dry-air partial column averaged mole fractions  $X_{CO,p}$  in the vertical range of surface-8 km and 8-20 km following Eq. 2.

$$X_{CO,p} = PC_{CO,p}/PC_{air,p}^{dry} = PC_{CO,p}/(PC_{air,p}^{wet} - PC_{H_2O,p}), \quad (5)$$

where  $PC_{CO,p}$ ,  $PC_{H_2O,p}$ ,  $PC_{air,p}^{dry}$  and  $PC_{air,p}^{wet}$  are the partial column of CO,  $\text{H}_2\text{O}$ , dry air and wet air in that vertical range.

The in-situ CO measurements are compared in Figure 9 with the NDACC  $X_{CO,p}$  in the vertical range of surface-8 km and 8-20 km. As we expected, the R between the in-situ and NDACC  $X_{CO,p}$  in surface-8 km (0.81) is larger than the in-situ and NDACC  $X_{CO,p}$  in 8-20 km (0.50). The large R value and the slope close to 1.0 between the in-situ and NDACC  $X_{CO,p}$  in surface-8 km confirm that NDACC CO retrievals have a very good sensitivity to the lower troposphere. NDACC retrievals 5 show that air in the upper troposphere and the lower stratosphere also captures the signal from the biomass burning despite the weaker peak. In general, the peaks of CO at the surface, in surface-8 km and in 8-20 km all occur in September–November, which are dominated by the biomass burning emission.

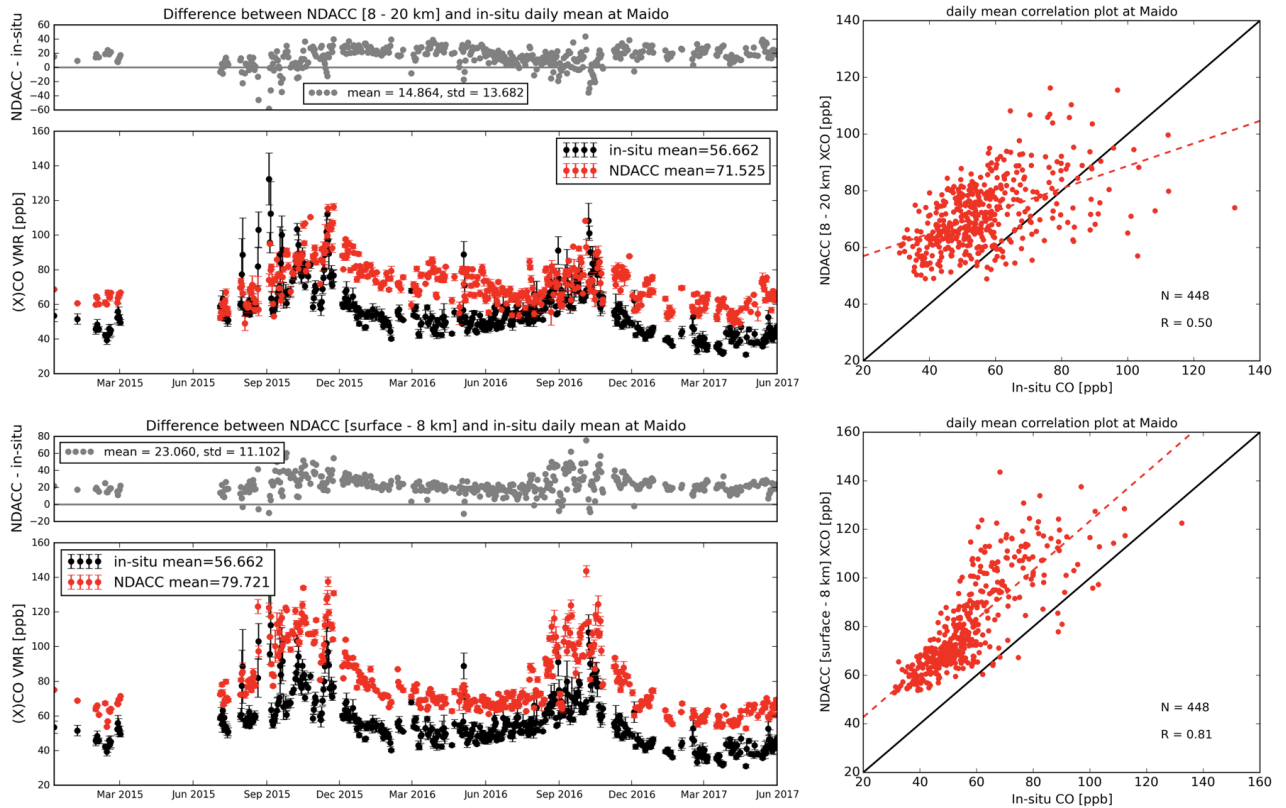


**Figure 9.** The time series of the daily means and standard deviations from the daytime in-situ CO measurements and NDACC  $X_{CO}$  in vertical range of 8-20 km (upper panels) and surface-8 km (lower panels) at Maido, together with the absolute difference (unit: ppb) between them (left panels) and their correlation (right panels).

## 4.2 CH<sub>4</sub>

### 4.2.1 Different seasonal cycles in the troposphere and stratosphere

In section 3.3, we found that the seasonal cycles of CH<sub>4</sub> from the in-situ and FTIR measurements are different. Ostler et al. (2016) pointed out that the stratospheric CH<sub>4</sub> has an important contribution to the variation of the total column, and the NDACC

5 CH<sub>4</sub> retrievals have the ability to get two individual information for the troposphere and the stratosphere. Therefore, in this section, we separate the total column into tropospheric and stratospheric parts. Figure 10 shows the tropopause height above Reunion Island from the NCEP re-analysis data for 2000-2016. The tropopause height is about 16-17 km with the maximum in February-April and minimum in August-October. The in-situ measurements are treated as the reference to compare with the FTIR retrievals in the troposphere.

10 For NDACC retrieved CH<sub>4</sub> profiles, similar to  $X_{CO,p}$  (Eq. 5), we calculate the dry-air column averaged mole fractions of CH<sub>4</sub> in the troposphere ( $X_{CH_4,tr}$ ) and stratosphere ( $X_{CH_4,st}$ ), respectively.

$$X_{CH_4,tr} = PC_{CH_4,tr}/PC_{air,tr}^{dry} = PC_{CH_4,tr}/(PC_{air,tr}^{wet} - PC_{H_2O,tr}), \quad (6)$$

$$X_{CH_4,st} = PC_{CH_4,st}/PC_{air,st}^{dry}, \quad (7)$$

15 where  $PC_{CH_4,tr}$ ,  $PC_{H_2O,tr}$ ,  $PC_{air,tr}^{dry}$  and  $PC_{air,tr}^{wet}$  are the partial column of CH<sub>4</sub>, H<sub>2</sub>O, dry air and wet air in the troposphere;  $PC_{CH_4,st}$  and  $PC_{air,st}^{dry}$  are the partial column of CH<sub>4</sub> and dry air in the stratosphere. Note that the H<sub>2</sub>O partial column in the stratosphere is ignored as H<sub>2</sub>O concentration is very low at high altitude. We take the vertical range from the surface to 16.5 km as the troposphere and from 16.5 to 60 km as the stratosphere above Reunion Island.

20 For TCCON X<sub>CH<sub>4</sub></sub> retrievals, it is not straightforward to separate the total column into tropospheric and stratospheric parts, because GGG2014 uses scaling profile retrieval method. Fortunately, previous studies have proved that the HF total column (Washenfelder et al., 2003) or the stratospheric N<sub>2</sub>O (Wang et al., 2014) could be used as an estimator to get the tropospheric CH<sub>4</sub>, since there is a good relationship between the CH<sub>4</sub> and HF or N<sub>2</sub>O in the stratosphere. The HF and N<sub>2</sub>O total columns are also retrieved from the TCCON spectra by GGG2014. However, the retrieved HF is seriously affected by the H<sub>2</sub>O concentration, especially at a humid site such as St Denis. Therefore, we use the N<sub>2</sub>O column to calculate the stratospheric CH<sub>4</sub> and the tropospheric CH<sub>4</sub>. The relationship between the stratospheric CH<sub>4</sub> and N<sub>2</sub>O is derived from the ACE-FTS satellite data. For a thorough description of the N<sub>2</sub>O proxy method, refer to Wang et al. (2014).

25 In the stratosphere, the MIPAS satellite observations are applied to compare with the FTIR retrievals ( $X_{CH_4,st}$ ). MIPAS observed the global distributions of CH<sub>4</sub> profiles for 2002-2012 using the limb sounding technique. MIPAS performed a full spectral resolution mode (FR) with a spectral resolution of 0.05 cm<sup>-1</sup> from July 2002 to March 2004. After that, one of the interferometer sides was broken, and MIPAS switched to a reduced spectral resolution mode (RR) with a spectral resolution of 0.121 cm<sup>-1</sup> (Fischer et al., 2008). In this section, we use the MIPAS level-2 version V5H (FR) and V5R (RR) data from the Institut für Meteorologie und Klimaforschung/Instituto de Astrofísica de Andalucía (von Clarmann et al., 2003). The MIPAS

CH<sub>4</sub> profile covers the upper troposphere and the whole stratosphere (about 12-70 km). The DOFs of CH<sub>4</sub> profile retrieved from MIPAS measurements is about 12 with a vertical resolution of 3-5 km below 50 km and 6-10 km above 50 km. The MIPAS observations in the vertical range of 16.5-60 km around Reunion Island within  $\pm 3^\circ$  latitude and  $\pm 5^\circ$  longitude are selected for comparison with the FTIR retrievals in the same vertical range. MIPAS observations show that the CH<sub>4</sub> concentration 5 decreases with increasing altitude in the stratosphere.

The NDACC retrievals at St Denis for 2004-2011 are also analysed in this section, because the MIPAS instrument stopped in the spring of 2012. According to Rodgers (2003), the vertical sensitivity should be taken into account when comparing two remote sensing retrievals. As the vertical resolution of MIPAS observation is higher than that of FTIR measurement, the smoothing correction was carried out for the MIPAS profiles.

$$10 \quad PC'_M = PC_{a,N} + A(\mathbf{P}_M - \mathbf{P}_{a,N}), \quad (8)$$

where  $\mathbf{P}_{a,N}$  and  $\mathbf{P}_M$  are the NDACC a priori partial column profile and MIPAS retrieved partial column profile, respectively;  $PC_{a,N}$  is the NDACC a priori partial column (16.5-60 km);  $PC'_M$  is the smoothed MIPAS retrieved partial column (16.5-60 km);  $A$  is the partial column (16.5-60 km) averaging kernel of NDACC retrieval at St Denis. The  $X_{CH_4,st}$  from the MIPAS measurements are calculated to compare with the FTIR retrievals quantitatively, using Eq. 7.

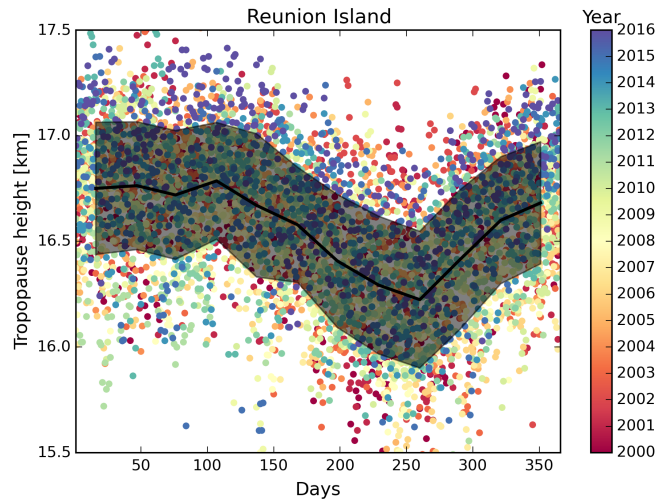


**Figure 10.** The tropopause height monthly means along with their uncertainties ( $1\sigma$ ) from the NCEP re-analysis data for 2000-2016 above Reunion Island.

15 Figure 11 shows the time series and seasonal cycles of CH<sub>4</sub> in the troposphere and stratosphere from the in-situ, FTIR (NDACC and TCCON) and MIPAS (with and without smoothing correction) measurements. In the stratosphere, the difference between NDACC and TCCON retrievals is less than 0.5%, which is within their measurement uncertainties. The MIPAS observations are slightly larger (about 30 ppb) compared to the NDACC measurement. The difference between MIPAS and NDACC

measurements is within their error budget, as the averaged measurement uncertainty of MIPAS partial columns in the vertical range of 16.5-60 km is 3.5% ( $\sim 50$  ppb). The seasonal cycles of stratospheric  $\text{CH}_4$  from all measurements show a maximum in March-April and a minimum in August-October. Since  $\text{CH}_4$  has a strong gradient near the tropopause, the seasonality is indicative of stratosphere troposphere exchange and circulation in the near tropopause region (Park et al., 2004a). The pattern of stratospheric  $\text{X}_{\text{CH}_4,st}$  seasonal cycle is highly related to the tropopause height (see Figure 10), and the tropopause height is dominated by the vertical transport (Holton et al., 1995). The enhanced  $\text{CH}_4$  concentration during March-April could be due to the convection which lifts air from the troposphere to the stratosphere. The minimum in August-October comes from the strengthened sink down in the stratosphere. In August-October the upwelling branch of the Brewer-Dobson circulation moves to the northern hemisphere and the sink down motion occurs in the stratosphere above Reunion (Seviour et al., 2012). The amplitudes of the seasonal cycles from the TCCON and MIPAS measurements are about  $\pm 40$  ppb, which are lower than the ones derived from NDACC measurements (about  $\pm 60$  ppb). The AVK (the red line in the right panel of Figure 3) shows that the retrieved partial column in the stratosphere from the NDACC retrieval overestimates the change in the stratosphere (AVK is about 1.3). After the smoothing correction, the amplitude of the seasonal cycle from the MIPAS measurements comes very close to the ones from the NDACC retrievals at the two sites.

In the troposphere, the seasonal cycles of  $\text{CH}_4$  from the in-situ and the FTIR (both NDACC and TCCON) measurements have the same pattern with the maximum in August-September and minimum in December-January, which is highly related to the OH seasonal variation (Bloss et al., 2005). In addition, all the amplitudes of the seasonal cycles are about  $\pm 10$  ppb. The  $\text{CH}_4$  concentration from the in-situ measurements at St Denis and Maïdo are very close. However, the in-situ measurement is on average about 17 ppb lower than the TCCON  $\text{X}_{\text{CH}_4,tr}$  and about 27 ppb lower than the NDACC  $\text{X}_{\text{CH}_4,tr}$ . In the next section, the simulations from the GEOS-Chem model are used to understand the difference observed in absolute levels between the in-situ, NDACC and TCCON  $\text{CH}_4$  measurements in the troposphere.

#### 4.2.2 GEOS-Chem model simulations in the troposphere

The 3-D Chemistry Transport Model GEOS-Chem (Wecht et al., 2014) is applied to investigate the seasonal cycle of methane in the troposphere and the differences between the in-situ and the FTIR measurements of tropospheric  $\text{CH}_4$ . This model is able to simulate the global vertical distributions of trace gases and aerosols. The methane offline simulation is performed with GEOS-Chem version 11-01, driven here by MERRA-2 reanalysis meteorological fields produced by the Global Modeling and Assimilation Office (GMAO) at the Goddard Space Flight Center. OH fields are prescribed from a 3-D archive of monthly mean OH concentrations (Park et al., 2004b), and the methane loss is augmented by soil absorption (Fung et al., 1991). The methane emissions are computed at run time by the HEMCO module (Harvard-NASA Emission Component; Keller et al. (2014)), notably accounting for the EDGAR v4.2 anthropogenic emissions inventory which includes oil and gas, coal mining, livestock, waste, residential biofuel emissions (European Commission, 2011) and the GFED4 biomass burning inventory (Randerson et al., 2015). We refer to Wecht et al. (2014) and Turner et al. (2015) for a description of the supplemental methane emission sources implemented in GEOS-Chem.

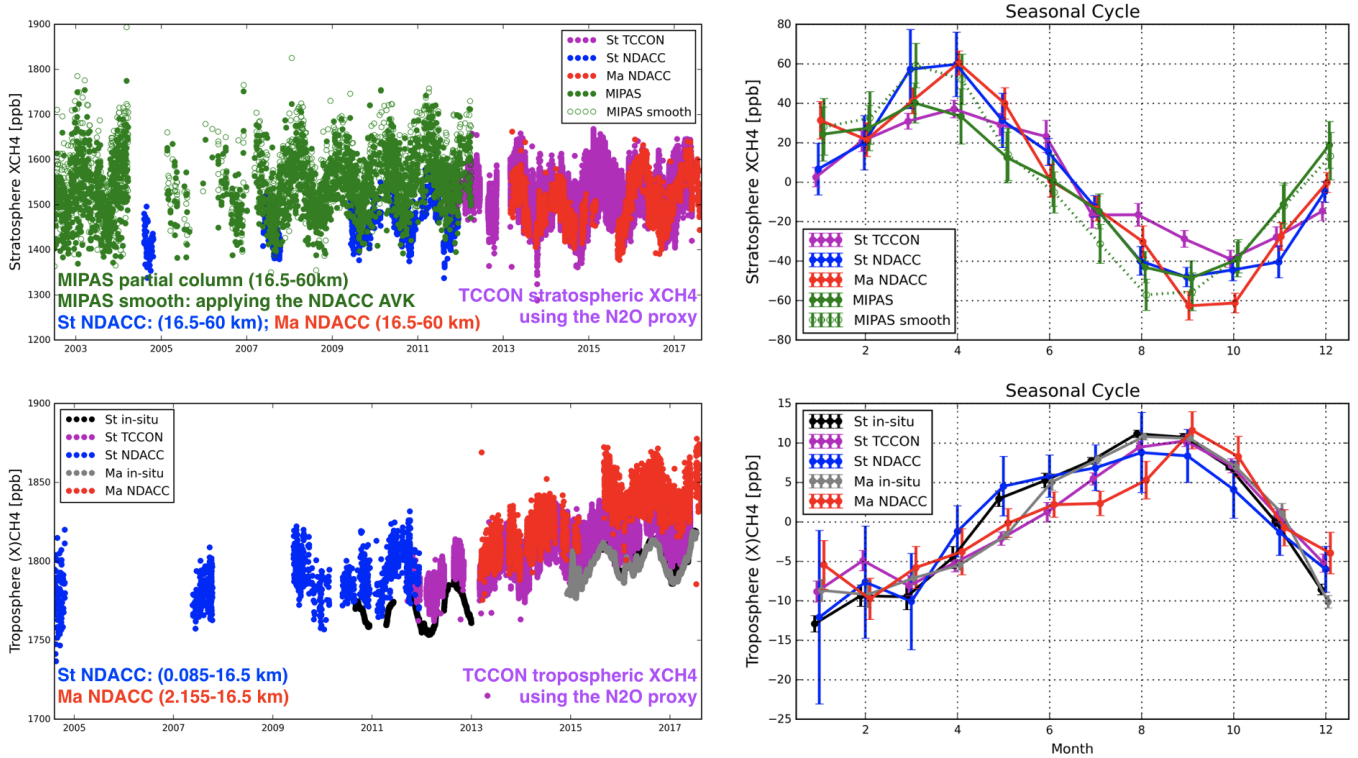


**Figure 11.** The time series and seasonal cycles of  $\text{CH}_4$  from the in-situ, FTIR (NDACC and TCCON) and co-located MIPAS measurements. Upper left: the time series of the stratospheric  $X_{\text{CH}_4}$  from the TCCON retrievals (the  $\text{N}_2\text{O}$  proxy method) at St Denis, NDACC and collocated MIPAS partial columns (16.5-60 km), together with the smoothed MIPAS measurements using the St Denis NDACC AVK. Upper right: the seasonal cycles of all the data in the stratosphere. Lower left: the time series of the tropospheric ( $X$ ) $\text{CH}_4$  from the in-situ measurements at St Denis and Maïdo, NDACC retrievals at St Denis (0.085-16.5 km) and Maïdo (2.155-16.5 km), and TCCON retrievals (the  $\text{N}_2\text{O}$  proxy method) at St Denis. Lower right: the seasonal cycles of the available data in the troposphere.

The whole year 2004 was used to spin-up the model simulation, adopting a  $2^\circ \times 2.5^\circ$  horizontal resolution and 47 levels, merging the levels above about 80 hPa. The simulation was subsequently extended to cover the 2005-2011 time period. The GEOS-Chem outputs are saved every three hours, and a mass-conservative interpolation provides re-gridded methane profiles on the NDACC retrieval altitude scheme (see section 3.1.1 in Bader et al. (2017)). These GEOS-Chem profiles are eventually 5 smoothed with the NDACC averaging kernels to ensure a fair comparison with the methane measurements (Rodgers, 2003).

Figure 12 compares the tropospheric measurements and the model results for the year 2011 at St Denis, the site and year for which all the measurement types are available. For the model simulation, surface  $\text{CH}_4$  as well as the smoothed  $X_{\text{CH}_4}$  in the troposphere (using the NDACC tropospheric partial column averaging kernel in the 0.085-16.5 km altitude range) are compared with the in-situ, NDACC and TCCON measurements, respectively. We did not apply the smoothing correction for 10 model simulations with the TCCON AVK, because 1) TCCON only provides the AVK for the total column, and we are looking

at the tropospheric partial column; 2) Using the TCCON total column AVK to correct the smoothing error in the vertical range of surface-16.5 km has also been tested, and the averaged difference between the smoothed and unsmoothed model data is within 0.5 ppb, which is much smaller than that for the NDACC data. The reason is that the a priori profile of TCCON is very close to the model simulation.

5 The smoothed  $X_{CH_4}$  from GEOS-Chem model is on average 11.5 ppb larger than the  $X_{CH_4}$  without smoothing. This is because the NDACC retrieved partial column in the troposphere is mostly sensitive to the vertical range of 5-13 km (see the blue line in the right panel of Figure 3) and the modelled  $CH_4$  mixing ratios are larger by 15-30 ppb in this layer, when compared to surface concentrations. As a result, the NDACC retrieved  $X_{CH_4}$  is larger than the TCCON retrievals in the troposphere. The GEOS-Chem simulation exhibit a clear seasonal modulation, with the maximum/minimum concentrations in  
10 August-September/December-January, primarily influenced by the OH variation throughout the year. It further indicates that the averaged  $CH_4$  VMR at the surface is 16.7 ppb lower than the tropospheric  $X_{CH_4}$  (without smoothing), in good agreement with the in-situ and TCCON measurements. To summarize, the model simulation captures the differences between in-situ and FTIR measurements (both NDACC and TCCON) as well as the seasonal variation of methane in the troposphere. Apart  
15 from that, two obvious spikes of  $CH_4$  were simulated by the GEOS-Chem model in January and February and one of them was also observed by NDACC retrievals on 02 February 2011. The FLEXPART backward trajectories computed for this time period demonstrate that these were due to transport of air masses from the northern hemisphere to Reunion Island (see Figure A2). Figure A1 also shows that air parcels over Reunion Island during the local summer time (December-February) are partly coming from the northern hemisphere indicating that the Intertropical Convergence Zone (ITCZ) sometimes moves south over Reunion Island.

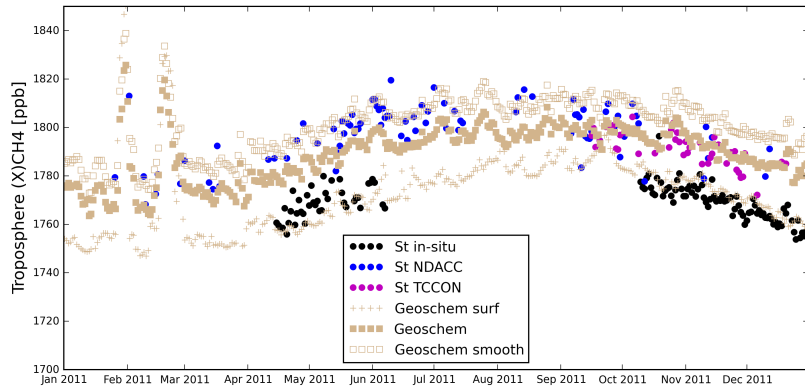


**Figure 12.** The time series of  $CH_4$  daily means from the in-situ measurements (black dots), NDACC tropospheric  $X_{CH_4}$  (blue dots) and TCCON tropospheric  $X_{CH_4}$  (purple dots) at St Denis, together with the GEOS-Chem model simulations of the VMR at the surface (brown cross), tropospheric  $X_{CH_4}$  (brown filled squares) and tropospheric  $X_{CH_4}$  after smoothing with NDACC AVK (brown empty squares) in 2011.

## 5 Conclusions

Atmospheric CO and CH<sub>4</sub> concentrations are measured by the in-situ and the FTIR instruments at two observatories (St Denis and Maïdo) on Reunion Island in the Indian Ocean. One Bruker IFS 125HR and one CRDS analyzer are currently operated at each site. The in-situ measurements provide the CO and CH<sub>4</sub> VMR at the surface, while the FTIR techniques observe the 5 abundance in the whole atmosphere along the solar light path. The FTIR at St Denis records NIR spectra, contributing to the TCCON network, while the FTIR at Maïdo records MIR spectra, contributing to the NDACC network.

The X<sub>CO</sub> from the FTIR retrievals are compared with in-situ measurements. The CO seasonal cycles observed from the in-situ and NDACC and TCCON measurements are in good agreement with the maximum in September-November and minimum in February-April. The CO maximum observed by both surface and total column measurements in September-November 10 corresponds to the biomass burning period in Africa and South America. The NDACC CO retrievals have a strong sensitivity in the lower and middle troposphere, and a good correlation ( $R=0.81$ ) is found between the co-located daily means from the in-situ and NDACC partial column-averaged X<sub>CO</sub> in the vertical range from surface to 8 km. The averaged X<sub>CO</sub> from NDACC retrievals is 15.7 ppb larger than the CO from in-situ measurements at Maïdo. The different CO concentration between the 15 surface and total column is related to the source of air on the Reunion Island. FLEXPART simulations show that, during the entire year, the air near the surface is mainly coming from the Indian Ocean and partly from Southern Africa, while the air in the middle and upper troposphere is mainly from Africa and South America. The CO concentration from the ocean is much lower than that from the land. As a result, the X<sub>CO</sub> from FTIR measurements at Maïdo is about 15.7 ppb systematically larger than the CO at the surface from in-situ measurements.

The trend of CH<sub>4</sub> is  $7.6 \pm 0.4$  ppb/year from the TCCON measurements for 2011-2017, which is consistent with the one of 20  $7.4 \pm 0.5$  ppb/year from the in-situ measurements for the same time period at St Denis. However, the seasonal cycles of CH<sub>4</sub> from the in-situ and FTIR measurements are very different. The CH<sub>4</sub> concentration decreases rapidly with altitude above the tropopause height ( $\sim 16.5$  km on Reunion Island) and the stratospheric CH<sub>4</sub> is vital for computing the total column of CH<sub>4</sub>. According to the AVK, both NDACC and TCCON retrieved X<sub>CH<sub>4</sub></sub> have a good sensitivity to the troposphere and stratosphere. 25 Therefore, the CH<sub>4</sub> seasonal cycles in the troposphere and stratosphere are analysed separately, based on the in-situ, FTIR measurements and the co-located MIPAS satellite observations. A very good agreement is observed in the tropospheric and stratospheric CH<sub>4</sub> seasonal cycles between FTIR (NDACC and TCCON) measurements, and in-situ and MIPAS measurements, respectively. In the troposphere, CH<sub>4</sub> VMR is high in August-September and low in December-January, which is highly related to the OH seasonal variation. In the stratosphere, CH<sub>4</sub> concentrations show the maximum in March-April and the minimum in August-October, which is dominated by vertical transport.

30 Finally, a simulation from the GEOS-Chem model in 2011 is used to understand the differences observed in absolute levels between the in-situ, NDACC and TCCON CH<sub>4</sub> measurements in the troposphere. The GEOS-Chem modelled CH<sub>4</sub> mixing ratios are larger by 15-30 ppb in the middle and upper troposphere (4-16 km), when compared to surface concentrations. As a result, GEOS-Chem X<sub>CH<sub>4</sub></sub> in the troposphere is 16.7 ppb larger than the CH<sub>4</sub> at the surface, which is in line with the difference between the in-situ and TCCON measurements. The difference between NDACC and TCCON retrieved X<sub>CH<sub>4</sub></sub> is mainly due

to the difference in vertical sensitivity. The averaged smoothed model simulation using the NDACC AVK is 11.5 ppb larger than the one without smoothing, which explains the difference between the NDACC and TCCON retrievals. In general, the in-situ, NDACC and TCCON measurements are in good agreement with the GEOS-Chem model simulation.

## 6 Data availability

5 The TCCON data at St Denis are publicly available through the TCCON wiki (De Maziere et al., 2017). The NDACC data at St Denis and Maïdo are publicly available from the NDACC database (<ftp://ftp.cpc.ncep.noaa.gov/ndacc/>). The in-situ measurements on Reunion Island are not publicly available yet, which can be obtained by contacting the authors. The MIPAS satellite observations are publicly available from KIT/IMK (<https://www.imk-asf.kit.edu/english/308.php>). The GEOS-Chem model data can be obtained from Emmanuel Mahieu ([emmanuel.mahieu@uliege.be](mailto:emmanuel.mahieu@uliege.be)).

10 *Acknowledgements.* Harmonization and characterization of the NDACC and TCCON data have been supported by the EU FP7 project QA4ECV and H2020 project GAIA-CLIM. Minqiang Zhou is supported by the Belgian Complementary Researchers program. The TCCON site at Reunion Island is operated by the Royal Belgian Institute for Space Aeronomy with financial support in 2014, 2015, 2016 and 2017 under the EU project ICOS-Inwire and the ministerial decree for ICOS (FR/35/IC2) and local activities supported by LACy/UMR8105, Université de La Réunion. The surface measurements are supported by the SNO RAMCES/ICOS-France. We would like to thank E. De Watcher 15 (BIRA-IASB) for helpful discussions, B. Dils, F. Scolas (BIRA-IASB) for their contribution to the FTIR measurements, and C. Vuillemin, D. Combaz, R. Jacob, J. Marais (LSCE) for their contribution to the in-situ instruments maintenance. The authors also wish to thank the European Communities, the Région Réunion, CNRS, and Université de la Réunion for their support and contribution in the construction phase 20 of the research infrastructure OPAR. OPAR is presently funded by CNRS (INSU) and Université de La Réunion and managed by OSU-R (Observatoire des Sciences de l'Univers de La Réunion, UMS 3365). This work has been supported by the German Research Foundation (DFG, project PA 1714/2-2). The MERRA-2 data used in this study have been provided by the Global Modeling and Assimilation Office (GMAO) at NASA Goddard Space Flight Center. Whitney Bader received funding from the European Union's Horizon 2020 research and innovation programme under the Marie Skłodowska-Curie grant agreement no. 704951. The GEOS-Chem methane simulation at University of Liège was partly supported by the F.R.S. – FNRS (Brussels), under Grant J.0093.15. Emmanuel Mahieu is a Research Associate with F.R.S. – FNRS.

## Appendix A: FLEXPART backward simulation

The Lagrangian particle dispersion model FLEXPART v9.02 is capable to simulate a large range of atmospheric transport processes, taking into account mean flow, deep convection, and turbulence (Stohl et al., 2005). The backward simulation of FLEXPART provides the release-receptor relationship, which is applied to study the source and transport of the observations 5 from a measurement site. In this study, air particles are released over Reunion Island at four vertical ranges in the troposphere, and a four-dimensional response function (sensitivity) to emission inventory is calculated. The model was driven by the meteorological data from the European Centre for Medium Range Weather Forecast (ECMWF). The residence time of particles in output grid cells describes the sensitivity of the receptor to the source. The detail settings of the FLEXPART backward run are listed in the Table A1.

**Table A1.** The settings of FLEXPART v9.02 backward simulation used in this study.

Input meteorological data	ECMWF data at $1^\circ \times 1^\circ$ global
Tracer	Air
Release location horizontal	$\pm 0.2^\circ$ latitude/longitude around Reunion Island
Release location vertical	0-2000, 4000-6000, 8000-10000, 12000-14000 m a.s.l.
Release time	06:00-18:00 local time for each day from 2011 to 2013
Number of days for backward running	20 days
Number of particles for each release	20000
Output grid Horizontal	$1^\circ \times 1^\circ$ global
Output grid vertical	0-16000 m a.s.l.

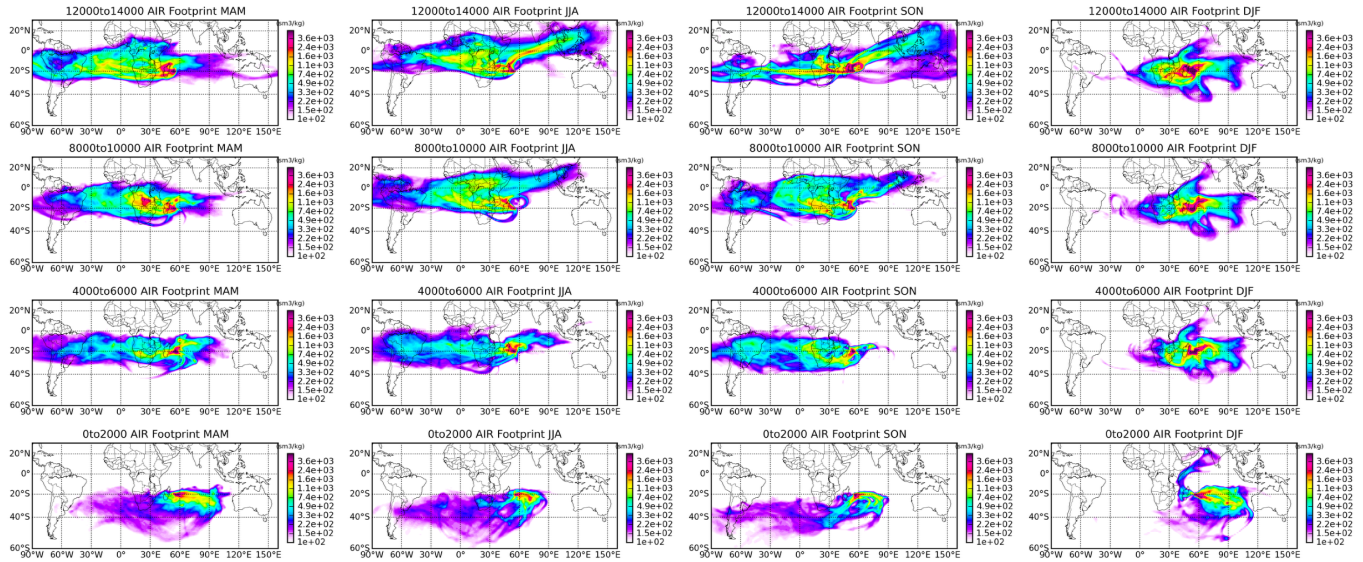


**Figure A1.** Seasonal distributions of the emission response sensitivity in backward simulations of the air at four vertical ranges (0-2000; 4000-6000; 8000-10000; 12000-14000 m a.s.l.) in the troposphere above Reunion Island in 2011-2013 simulated with FLEXPART v9.02 (20 days' backward running). Sensitivity is given in units of  $\text{sm}^3 \text{kg}^{-1}$ .

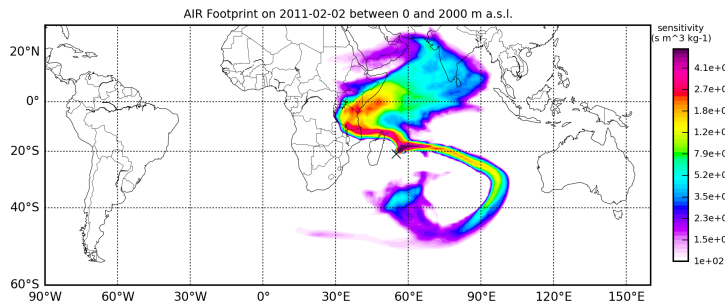


**Figure A2.** The emission response sensitivity of the air mass above Reunion Island in the vertical range of 0-2000 m a.s.l. on February 2, 2011 simulated with a 20 days' backward run by FLEXPART v9.02.

## References

Aschi, M. and Largo, A.: Reactivity of gaseous protonated ozone: A computational investigation on the carbon monoxide oxidation reaction, *Int. J. Mass Spectrom.*, doi:10.1016/S1387-3806(03)00134-9, 2003.

Bader, W., Bovy, B., Conway, S., Strong, K., Smale, D., Turner, A. J., Blumenstock, T., Boone, C., Collaud Coen, M., Coulon, A., Garcia, 5 O., Griffith, D. W. T., Hase, F., Hausmann, P., Jones, N., Krummel, P., Murata, I., Morino, I., Nakajima, H., O'Doherty, S., Paton-Walsh, C., Robinson, J., Sandrin, R., Schneider, M., Servais, C., Sussmann, R., and Mahieu, E.: The recent increase of atmospheric methane from 10 years of ground-based NDACC FTIR observations since 2005, *Atmos. Chem. Phys.*, 17, 2255–2277, doi:10.5194/acp-17-2255-2017, 2017.

Baray, J. L., Courcoux, Y., Keckhut, P., Portafaix, T., Tulet, P., Cammas, J. P., Hauchecorne, A., Godin Beekmann, S., De Mazière, M., 10 Hermans, C., Desmet, F., Sellegri, K., Colomb, A., Ramonet, M., Sciare, J., Vuillemin, C., Hoareau, C., Dionisi, D., Duflot, V., Vérèmes, H., Porteneuve, J., Gabarrot, F., Gaudio, T., Metzger, J. M., Payen, G., Leclair De Bellevue, J., Barthe, C., Posny, F., Ricaud, P., Abchiche, A., and Delmas, R.: Maïdo observatory: A new high-altitude station facility at Reunion Island (21 S, 55 E) for long-term atmospheric remote sensing and in situ measurements, *Atmos. Meas. Tech.*, doi:10.5194/amt-6-2865-2013, 2013.

Birk, M., Wagner, G., Loos, J., Lodi, L., Polyansky, O. L., Kyuberis, A. A., Zobov, N. F., and Tennyson, J.: Accurate line intensities for water transitions in the infrared: Comparison of theory and experiment, *J. Quant. Spectrosc. Radiat. Transf.*, 203, 88–102, 15 doi:10.1016/J.JQSRT.2017.03.040, 2017.

Bloss, W. J., Evans, M. J., Lee, J. D., Sommariva, R., Heard, D. E., and Pilling, M. J.: The oxidative capacity of the troposphere: Coupling of field measurements of OH and a global chemistry transport model, *Faraday Discuss.*, doi:10.1039/b419090d, 2005.

Cullis, C. F. and Willatt, B. M.: Oxidation of methane over supported precious metal catalysts, *J. Catal.*, doi:10.1016/0021-9517(83)90054-4, 20 1983.

De Maziere, M., Sha, M. K., Desmet, F., Hermans, C., Scolas, F., Kumps, N., Metzger, J.-M., Duflot, V., and Cammas, J.-P.: TCCON data from Reunion Island (La Reunion), France, Release GGG2014R0. TCCON data archive, hosted by CaltechDATA, California Institute of Technology, Pasadena, CA, U.S.A. , <https://doi.org/10.14291/tccon.ggg2014.reunion01.R0/1149288>, 2017.

Deeter, M. N., Martínez-Alonso, S., Edwards, D. P., Emmons, L. K., Gille, J. C., Worden, H. M., Sweeney, C., Pittman, J. V., Daube, 25 B. C., and Wofsy, S. C.: The MOPITT Version 6 product: Algorithm enhancements and validation, *Atmos. Meas. Tech.*, 7, 3623–3632, doi:10.5194/amt-7-3623-2014, 2014.

Dils, B., Cui, J., Henne, S., Mahieu, E., Steinbacher, M., and De Mazière, M.: 1997–2007 CO trend at the high Alpine site Jungfraujoch: a comparison between NDIR surface in situ and FTIR remote sensing observations, *Atmos. Chem. Phys.*, 11, 6735–6748, doi:10.5194/acp-11-6735-2011, 2011.

Duflot, V., Dils, B., Baray, J. L., De Mazière, M., Attié, J. L., Vanhaelewyn, G., Senten, C., Vigouroux, C., Clain, G., and Delmas, R.: 30 Analysis of the origin of the distribution of CO in the subtropical southern Indian Ocean in 2007, *J. Geophys. Res. Atmos.*, 115, 1–16, doi:10.1029/2010JD013994, 2010.

European Commission, .: Emission Database for Global Atmospheric Research (EDGAR), release version 4.2, Tech. rep., Joint Research Centre (JRC)/Netherlands Environmental Assessment Agency (PBL) last access: 22 February 2018, <http://edgar.jrc.ec.europa.eu>, 2011.

Fischer, H., Birk, M., Blom, C., Carli, B., Carlotti, M., von Clarmann, T., Delbouille, L., Duhia, A., Ehhalt, D., Endemann, M., Flaud, 35 J. M., Gessner, R., Kleinert, A., Koopman, R., Langen, J., López-Puertas, M., Mosner, P., Nett, H., Oelhaf, H., Perron, G., Remedios, J.,

Ridolfi, M., Stiller, G., and Zander, R.: MIPAS: an instrument for atmospheric and climate research, *Atmos. Chem. Phys.*, 8, 2151–2188, doi:10.5194/acp-8-2151-2008, 2008.

Folini, D., Kaufmann, P., Ubl, S., and Henne, S.: Region of influence of 13 remote European measurement sites based on modeled carbon monoxide mixing ratios, *J. Geophys. Res. Atmos.*, doi:10.1029/2008JD011125, 2009.

5 Fung, I., John, J., Lerner, J., Matthews, E., Prather, M., Steele, L. P., and Fraser, P. J.: Three-dimensional model synthesis of the global methane cycle, *J. Geophys. Res.*, 96, 13 033, doi:10.1029/91JD01247, 1991.

Hazan, L., Tarniewicz, J., Ramonet, M., Laurent, O., and Abbaris, A.: Automatic processing of atmospheric CO<sub>2</sub> and CH<sub>4</sub> mole fractions at the ICOS Atmosphere Thematic Centre, *Atmos. Meas. Tech.*, doi:10.5194/amt-9-4719-2016, 2016.

Holton, J. R., Haynes, P. H., McIntyre, M. E., Douglass, A. R., Rood, R. B., and Pfister, L.: Stratosphere-troposphere exchange, 10 doi:10.1029/95RG02097, 1995.

IPCC: Climate change 2013: The physical science basis. Contribution of Working Group I to the Fifth Assessment Report of the Intergovernmental Panel on Climate Change, 2013.

Kasischke, E. S. and Bruhwiler, L. P.: Emissions of carbon dioxide, carbon monoxide, and methane from boreal forest fires in 1998, *J. Geophys. Res. - Atmos.*, doi:10.1029/2001JD000461, 2002.

15 Keller, C. A., Long, M. S., Yantosca, R. M., Da Silva, A. M., Pawson, S., and Jacob, D. J.: HEMCO v1.0: A versatile, ESMF-compliant component for calculating emissions in atmospheric models, *Geosci. Model Dev.*, doi:10.5194/gmd-7-1409-2014, 2014.

Kiel, M., Hase, F., Blumenstock, T., and Kirner, O.: Comparison of XCO abundances from the Total Carbon Column Observing Network and the Network for the Detection of Atmospheric Composition Change measured in Karlsruhe, *Atmos. Meas. Tech.*, 9, 2223–2239, doi:10.5194/amt-9-2223-2016, 2016.

20 Kirschke, S., Bousquet, P., Ciais, P., Saunois, M., Canadell, J. G., Dlugokencky, E. J., Bergamaschi, P., Bergmann, D., Blake, D. R., Bruhwiler, L., Cameron-Smith, P., Castaldi, S., Chevallier, F., Feng, L., Fraser, A., Heimann, M., Hodson, E. L., Houweling, S., Josse, B., Fraser, P. J., Krummel, P. B., Lamarque, J.-F., Langenfelds, R. L., Le Quéré, C., Naik, V., O'Doherty, S., Palmer, P. I., Pison, I., Plummer, D., Poulter, B., Prinn, R. G., Rigby, M., Ringeval, B., Santini, M., Schmidt, M., Shindell, D. T., Simpson, I. J., Spahni, R., Steele, L. P., Strode, S. A., Sudo, K., Szopa, S., van der Werf, G. R., Voulgarakis, A., van Weele, M., Weiss, R. F., Williams, J. E., and Zeng, G.: Three decades of 25 global methane sources and sinks, *Nat. Geosci.*, doi:10.1038/ngeo1955, 2013.

Laurent, O.: ICOS Atmospheric Station Specifications, [https://icos-atc.lsce.ipsl.fr/doc\\_public](https://icos-atc.lsce.ipsl.fr/doc_public), 2016.

Loos, J., Birk, M., and Wagner, G.: Measurement of air-broadening line shape parameters and temperature dependence parameters of H<sub>2</sub>O lines in the spectral ranges 1850–2280 cm<sup>-1</sup> and 2390–4000 cm<sup>-1</sup>, *J. Quant. Spectrosc. Radiat. Transf.*, 203, 103–118, doi:10.1016/J.JQSRT.2017.03.033, 2017a.

30 Loos, J., Birk, M., and Wagner, G.: Measurement of positions, intensities and self-broadening line shape parameters of H<sub>2</sub>O lines in the spectral ranges 1850–2280 cm<sup>-1</sup> and 2390–4000 cm<sup>-1</sup>, *J. Quant. Spectrosc. Radiat. Transf.*, 203, 119–132, doi:10.1016/J.JQSRT.2017.02.013, 2017b.

Lopez, M., Schmidt, M., Ramonet, M., Bonne, J. L., Colomb, A., Kazan, V., Laj, P., and Pichon, J. M.: Three years of semicontinuous greenhouse gas measurements at the Puy de Dôme station (central France), *Atmos. Meas. Tech.*, doi:10.5194/amt-8-3941-2015, 2015.

35 Messerschmidt, J., Geibel, M. C., Blumenstock, T., Chen, H., Deutscher, N. M., Engel, A., Feist, D. G., Gerbig, C., Gisi, M., Hase, F., Katrynski, K., Kolle, O., Lavrič, J. V., Notholt, J., Palm, M., Ramonet, M., Rettinger, M., Schmidt, M., Sussmann, R., Toon, G. C., Truong, F., Warneke, T., Wennberg, P. O., Wunch, D., and Xueref-Remy, I.: Calibration of TCCON column-averaged CO<sub>2</sub>: The first aircraft campaign over European TCCON sites, *Atmos. Chem. Phys.*, doi:10.5194/acp-11-10765-2011, 2011.

Novelli, P. C.: Reanalysis of tropospheric CO trends: Effects of the 1997–1998 wildfires, *J. Geophys. Res.*, doi:10.1029/2002JD003031, 2003.

Novelli, P. C., Masarie, K. A., and Lang, P. M.: Distributions and recent changes of carbon monoxide in the lower troposphere, *J. Geophys. Res. Atmos.*, doi:10.1029/98JD01366, 1998.

5 Ostler, A., Sussmann, R., Rettinger, M., Deutscher, N. M., Dohe, S., Hase, F., Jones, N., Palm, M., and Sinnhuber, B.-M.: Multistation intercomparison of column-averaged methane from NDACC and TCCON: impact of dynamical variability, *Atmos. Meas. Tech.*, 7, 4081–4101, doi:10.5194/amt-7-4081-2014, 2014.

Ostler, A., Sussmann, R., Patra, P. K., Houweling, S., De Bruine, M., Stiller, G. P., Haenel, F. J., Plieninger, J., Bousquet, P., Yin, Y., Saunois, M., Walker, K. A., Deutscher, N. M., Griffith, D. W. T., Blumenstock, T., Hase, F., Warneke, T., Wang, Z., Kivi, R., and Robinson, J.:  
10 Evaluation of column-averaged methane in models and TCCON with a focus on the stratosphere, *Atmos. Meas. Tech.*, 9, 4843–4859, doi:10.5194/amt-9-4843-2016, 2016.

Park, M., Randel, W. J., Kinnison, D. E., Garcia, R. R., and Choi, W.: Seasonal variation of methane, water vapor, and nitrogen oxides near the tropopause: Satellite observations and model simulations, *J. Geophys. Res. Atmos.*, doi:10.1029/2003JD003706, 2004a.

Park, R. J., Jacob, D. J., Field, B. D., Yantosca, R. M., and Chin, M.: Natural and transboundary pollution influences on sulfate-nitrate-  
15 ammonium aerosols in the United States: Implications for policy, *J. Geophys. Res. D Atmos.*, doi:10.1029/2003JD00473, 2004b.

Pougatchev, N. S., Connor, B. J., and Rinsland, C. P.: Infrared measurements of the ozone vertical distribution above Kitt Peak, *J. Geophys. Res.*, 100, 16 689, doi:10.1029/95JD01296, 1995.

Randerson, J. T., van der Werf, G. R., Giglio, L., Collatz, G. J., and Kasibhatla, P. S.: Global Fire Emissions Database, Version 4, (GFEDv4), doi:10.3334/ORNLDAC/1293, 2015.

20 Rasmussen, R. A. and Khalil, M. A. K.: Atmospheric methane (CH<sub>4</sub>): Trends and seasonal cycles, *J. Geophys. Res. Oceans*, 86, 9826–9832, doi:10.1029/JC086iC10p09826, 1981.

Rella, C. W., Chen, H., Andrews, A. E., Filges, A., Gerbig, C., Hatakka, J., Karion, A., Miles, N. L., Richardson, S. J., Steinbacher, M., Sweeney, C., Wastine, B., and Zellweger, C.: High accuracy measurements of dry mole fractions of carbon dioxide and methane in humid air, *Atmos. Meas. Tech.*, doi:10.5194/amt-6-837-2013, 2013.

25 Rigby, M., Prinn, R. G., Fraser, P. J., Simmonds, P. G., Langenfelds, R. L., Huang, J., Cunnold, D. M., Steele, L. P., Krummel, P. B., Weiss, R. F., O'Doherty, S., Salameh, P. K., Wang, H. J., Harth, C. M., Mühle, J., and Porter, L. W.: Renewed growth of atmospheric methane, *Geophys. Res. Lett.*, 35, L22 805, doi:10.1029/2008GL036037, 2008.

Rodgers, C. D.: Inverse Methods for Atmospheric Sounding – Theory and Practice, Series on Atmospheric Oceanic and Planetary Physics, vol. 2, World Scientific Publishing Co. Pte. Ltd, Singapore, doi:10.1142/9789812813718, 2000.

30 Rodgers, C. D.: Intercomparison of remote sounding instruments, *J. Geophys. Res.*, 108, 46–48, doi:10.1029/2002JD002299, 2003.

Senten, C., De Mazière, M., Dils, B., Hermans, C., Kruglanski, M., Neefs, E., Scolas, F., Vandaele, A. C., Vanhaelewijn, G., Vigouroux, C., Carleer, M., Coheur, P. F., Fally, S., Barret, B., Baray, J. L., Delmas, R., Leveau, J., Metzger, J. M., Mahieu, E., Boone, C., Walker, K. A., Bernath, P. F., and Strong, K.: Technical Note: New ground-based FTIR measurements at Ile de La Réunion: observations, error analysis, and comparisons with independent data, *Atmos. Chem. Phys.*, 8, 3483–3508, doi:10.5194/acp-8-3483-2008, 2008.

35 Sepúlveda, E., Schneider, M., Hase, F., Barthlott, S., Dubravica, D., García, O. E., Gomez-Pelaez, A., González, Y., Guerra, J. C., Gisi, M., Kohlhepp, R., Dohe, S., Blumenstock, T., Strong, K., Weaver, D., Palm, M., Sadeghi, A., Deutscher, N. M., Warneke, T., Notholt, J., Jones, N., Griffith, D. W. T., Smale, D., Brailsford, G. W., Robinson, J., Meinhardt, F., Steinbacher, M., Aalto, T., and Worthy, D.: Tropospheric

CH4 signals as observed by NDACC FTIR at globally distributed sites and comparison to GAW surface in situ measurements, *Atmos. Meas. Tech.*, 7, 2337–2360, doi:10.5194/amt-7-2337-2014, 2014.

Seviour, W. J. M., Butchart, N., and Hardiman, S. C.: The Brewer-Dobson circulation inferred from ERA-Interim, *Q. J. R. Meteorol. Soc.*, doi:10.1002/qj.966, 2012.

5 Stohl, A., Forster, C., Frank, A., Seibert, P., and Wotawa, G.: Technical note: The Lagrangian particle dispersion model FLEXPART version 6.2, *Atmos. Chem. Phys.*, 5, 2461–2474, doi:10.5194/acp-5-2461-2005, 2005.

Sussmann, R., Forster, F., Rettinger, M., and Bousquet, P.: Renewed methane increase for five years (2007–2011) observed by solar FTIR spectrometry, *Atmos. Chem. Phys.*, 12, 4885–4891, doi:10.5194/acp-12-4885-2012, 2012.

Té, Y., Jeseck, P., Franco, B., Mahieu, E., Jones, N., Paton-Walsh, C., Griffith, D. W. T., Buchholz, R. R., Hadji-Lazaro, J., Hurtmans, D., 10 and Janssen, C.: Seasonal variability of surface and column carbon monoxide over the megacity Paris, high-altitude Jungfraujoch and Southern Hemispheric Wollongong stations, *Atmos. Chem. Phys.*, 16, 10 911–10 925, doi:10.5194/acp-16-10911-2016, 2016.

Toon, G. C.: Telluric line list for GGG2014, TCCON data archive, hosted by the Carbon Dioxide Information Analysis Center, Oak Ridge National Laboratory, Oak Ridge, Tennessee, U.S.A., doi:10.14291/tccon.ggg2014.atm.R0/1221656, 2014.

Toon, G. C. and Wunch, D.: A stand-alone a priori profile generation tool for GGG2014 release, TCCON data archive, 15 hosted by the Carbon Dioxide Information Analysis Center, Oak Ridge National Laboratory, Oak Ridge, Tennessee, U.S.A., doi:10.14291/TCCON.GGG2014.PRIORS.R0/1221661, 2014.

Turner, A. J., Jacob, D. J., Wecht, K. J., Maasakkers, J. D., Lundgren, E., Andrews, A. E., Biraud, S. C., Boesch, H., Bowman, K. W., Deutscher, N. M., Dubey, M. K., Griffith, D. W., Hase, F., Kuze, A., Notholt, J., Ohyama, H., Parker, R., Payne, V. H., Sussmann, R., Sweeney, C., Velazco, V. A., Warneke, T., Wennberg, P. O., and Wunch, D.: Estimating global and North American methane emissions 20 with high spatial resolution using GOSAT satellite data, *Atmos. Chem. Phys.*, doi:10.5194/acp-15-7049-2015, 2015.

Vermeulen, A. T., Hensen, A., Popa, M. E., Van Den Bulk, W. C., and Jongejan, P. A.: Greenhouse gas observations from Cabauw Tall Tower (1992–2010), *Atmos. Meas. Tech.*, doi:10.5194/amt-4-617-2011, 2011.

Vigouroux, C., Stavrakou, T., Whaley, C., Dils, B., Duflat, V., Hermans, C., Kumps, N., Metzger, J. M., Scolas, F., Vanhaelewijn, G., Müller, 25 J. F., Jones, D. B. A., Li, Q., and De Mazière, M.: FTIR time-series of biomass burning products (HCN, C2H6, C2H2, CH3OH, and HCOOH) at Reunion Island (21 S, 55 E) and comparisons with model data, *Atmos. Chem. Phys.*, 12, 10 367–10 385, doi:10.5194/acp-12-10367-2012, 2012.

von Clarmann, T., Ceccherini, S., Doicu, A., Dudhia, A., Funke, B., Grabowski, U., Hilgers, S., Jay, V., Linden, A., Lopez-Puertas, M., Martin-Torres, F. J., Payne, V., Reburn, J., Ridolfi, M., Schreier, F., Schwarz, G., Siddans, R., and Steck, T.: A blind test retrieval experiment for infrared limb emission spectrometry, *J. Geophys. Res.*, doi:10.1029/2003jd003835, 2003.

30 Wang, Z., Deutscher, N. M., Warneke, T., Notholt, J., Dils, B., Griffith, D. W. T., Schmidt, M., Ramonet, M., and Gerbig, C.: Retrieval of tropospheric column-averaged CH4 mole fraction by solar absorption FTIR-spectrometry using N2O as a proxy, *Atmos. Meas. Tech.*, 7, 3295–3305, doi:10.5194/amt-7-3295-2014, 2014.

Washenfelder, R. A., Wennberg, P. O., and Toon, G. C.: Tropospheric methane retrieved from ground-based near-IR solar absorption spectra, *Geophys. Res. Lett.*, doi:10.1029/2003GL017969, 2003.

35 Wecht, K. J., Jacob, D. J., Frankenberg, C., Jiang, Z., and Blake, D. R.: Mapping of North American methane emissions with high spatial resolution by inversion of SCIAMACHY satellite data, *J. Geophys. Res.*, doi:10.1002/2014JD021551, 2014.

Wunch, D., Toon, G. C., Wennberg, P. O., Wofsy, S. C., Stephens, B. B., Fischer, M. L., Uchino, O., Abshire, J. B., Bernath, P., Biraud, S. C., Blavier, J. F. L., Boone, C., Bowman, K. P., Browell, E. V., Campos, T., Connor, B. J., Daube, B. C., Deutscher, N. M., Diao, M., Elkins,

J. W., Gerbig, C., Gottlieb, E., Griffith, D. W. T., Hurst, D. F., Jiménez, R., Keppel-Aleks, G., Kort, E. A., MacAtangay, R., MacHida, T., Matsueda, H., Moore, F., Morino, I., Park, S., Robinson, J., Roehl, C. M., Sawa, Y., Sherlock, V., Sweeney, C., Tanaka, T., and Zondlo, M. A.: Calibration of the total carbon column observing network using aircraft profile data, *Atmos. Meas. Tech.*, doi:10.5194/amt-3-1351-2010, 2010.

5 Wunch, D., Toon, G. C., Sherlock, V., Deutscher, N. M., Liu, C., Feist, D. G., and Wennberg, P. O.: The Total Carbon Column Observing Network's GGG2014 Data Version, p. 43, doi:10.14291, <http://dx.doi.org/10.14291/tccon.ggg2014.documentation.R0/1221662>, 2015.

Yang, Z., Toon, G. C., Margolis, J. S., and Wennberg, P. O.: Atmospheric CO<sub>2</sub> retrieved from ground-based near IR solar spectra, *Geophys. Res. Lett.*, 29, 53–1–53–4, doi:10.1029/2001GL014537, 2002.

Yokota, T., Yoshida, Y., Eguchi, N., Ota, Y., Tanaka, T., Watanabe, H., and Maksyutov, S.: Global Concentrations of CO<sub>2</sub> and CH<sub>4</sub> Retrieved  
10 from GOSAT: First Preliminary Results, *Sola*, doi:10.2151/sola.2009-041, 2009.

Yver Kwok, C., Laurent, O., Guemri, A., Philippon, C., Wastine, B., Rella, C. W., Vuillemin, C., Truong, F., Delmotte, M., Kazan, V., Dardignac, M., Lebègue, B., Kaiser, C., Xueref-Rémy, I., and Ramonet, M.: Comprehensive laboratory and field testing of cavity ring-down spectroscopy analyzers measuring H<sub>2</sub>O, CO<sub>2</sub>, CH<sub>4</sub> and CO, *Atmos. Meas. Tech.*, doi:10.5194/amt-8-3867-2015, 2015.

Zhou, M., Vigouroux, C., Langerock, B., Wang, P., Dutton, G., Hermans, C., Kumps, N., Metzger, J.-M., Toon, G., and De Mazière, M.: CFC-  
15 11, CFC-12 and HCFC-22 ground-based remote sensing FTIR measurements at Réunion Island and comparisons with MIPAS/ENVISAT data, *Atmos. Meas. Tech.*, 9, 5621–5636, doi:10.5194/amt-9-5621-2016, 2016.

Zhou, M., Langerock, B., Vigouroux, C., Wang, P., Hermans, C., Stiller, G., Walker, K. A., Dutton, G., Mahieu, E., and De Mazière, M.: Ground-based FTIR retrievals of SF<sub>6</sub> on Reunion Island, *Atmos. Meas. Tech.*, 11, 651–662, doi:10.5194/amt-11-651-2018, 2018.